Studies on Electron Transfer Pathway and Characterization of Direct Electron Transfer-Type Bioelectrocatalysis of Fructose Dehydrogenase

Shota Kawai

2015

Table of contents

General introduction

Electron transfer (ET) reactions are related to many biological processes, such as glycolysis process, tricarboxylic cycle, respiratory chain, and photosynthetic process [1,2]. Redox enzymes work as catalysts in these reactions. A limited kind of redox enzymes react directly with electrodes [3-5]. In other word, some redox enzymes are oxidized (or reduced) at electrodes. This reaction is called direct electron transfer (DET)-type bioelectrocatalysis. The DET reaction is a curious phenomenon. The cofactor in DET-type enzymes generally transfers electrons from (or to) electrodes. However, the cofactor is usually buried deeply inside the DET-type enzymes that consist of electric non-conductive folded polypeptide. This means that the tunnel (or long range) electron transfer occurs between electrodes and the cofactor in DET-type enzymes. There are many studies for controlling the distance between the active site in DET-type enzyme and the electrode surface [6,7-8].

The ET rate constant decays exponentially with increasing the distance between the redox centers according to Marcus theory [9]. When the theory is applied to the DET reaction, the DET rate constant is given as a function of the distance between the electrode surface and the redox center in DET-type enzymes. The DET reaction usually requires the adsorption of enzymes on the electrode surface at the proper orientation for DET reaction in order to shorten the distance between the electrode surface and the redox center. In addition, the property that the enzyme has more than two redox centers is essential to realize the DET-type bioelectrocatalysis [10]. When the enzyme has only one redox center and adsorbs on the electrode under the conditions that the redox center faces the electrode, the enzyme orientation is not convenient for the substrate to get close to the active site of the enzyme. There must exits another factors governing the DET reaction. However, it is extremely difficult to find novel common features among DET-type enzymes.

D-Fructose dehydrogenase (FDH) from *Gluconobacter japonicus* NBRC3260 (formerly *Gluconobacter industrius* IFO3260), which catalyzes the oxidation of D-fructose to produce 5-keto-D-fructose, is a heterotrimeric membrane-bound enzyme with a molecular mass of *ca.* 140 kDa, consisting of subunits I (67 kDa), II (51 kDa), and III (20 kDa). FDH was firstly discovered and purified by Ameyama group in 1981 [11]. FDH shows strict substrate specificity to D-fructose and is used in diagnosis and food analysis [12,13]. FDH is one of the DET-type enzymes. The DET ability is quite high [14]. Furthermore, FDH gives very large current density of

DET-type fructose oxidation at a large variety of electrodes [15-17]. However, the detail of the mechanism of DET reaction of FDH remains to be elucidated.

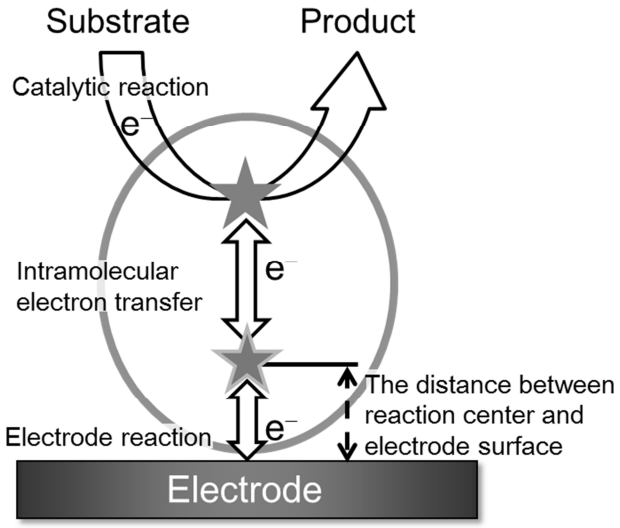

Figure 1. Schematic model of the ideal direct electron transfer pathway

In this research, to explore the mechanism of the DET reaction of FDH, the author has focused on factors that provide inconvenient influence on the DET ability of FDH. It is usually more difficult to improve the DET ability of enzymes than to worsen it. Therefore, if enzymes have only poor DET ability, it is very difficult to judge whether the DET ability is degraded or lost by some modifications. In contrast, it is high possibility to evaluate the influence of some modifications on the DET reaction of FDH, because the DET ability of FDH is quite high. The author has consider the conditions of the DET reaction of FDH from mainly two viewpoints. One is the enzymatic modification. The other is the electrode surface modification.

In chapter 1, the author has sequenced the genes encoding each subunit of the FDH complex from *G. japonicus* NBRC3260 and constructed an expression system to highly produce FDH in a *Gluconobacter oxydans* strain. In addition, the author has characterized the cofactors in each subunit of FDH.

In chapter 2, the author has constructed subunit I/III subcomplex (FdhSL) that lacks subunit II containing the three heme C moieties, and compared the electrochemical features with those of FDH. In addition, the author has determined the formal potentials ($E^{\circ\prime}$) of the three heme C moieties in FDH. These results were utilized to examine the ET pathway from FDH to electrodes. The author also evaluated the bi-molecular reaction rate constants (k) between FdhSL and

p-benzoquinone (*p*BQ) derivatives, and discussed the substrate specificity of FDH as an electron acceptor.

In chapter 3, the author has constructed an expression system of subunit II (FdhC) of FDH and attempted to observe the non-turnover signal from FdhC on cyclic voltammograms. FdhSL has been constructed in chapter 2. The author has demonstrated to repair catalytic DET activity of FdhSL by binding FdhC.

FDH required non-ionic surfactant in solubilization of membrane-bound FDH from the membrane fraction. However, it seems the surfactant prevents FDH from adsorbing on the electrode. In chapter 4, the author has focused his attention on effects of a non-ionic surfactant on the DET-type bioelectrocatalysis caused by FDH, and proposed a model of the adsorption of the surfactant and FDH to reasonably explain the experimental results.

References

[1] P. N. Bartlett (Ed), Bioelectrochemistry, John Wiley & Sons Ltd., West Sussex, 2008.

[2] G. W. Canters, and E. Vijgenboom (Eds), Biological Electron Transfer Chains: Genetics, Composition and Mode of Operation, Kluwer Academic Publishers, Dordrecht, 1998.

[3] A. L. Ghindilis, P. Atanasov, and E. Wilkins, Electroanalysis 9 (1997) 661.

[4] L. Gorton, A. Lindgren, T. Larsson, F. D. Munteanu, T. Ruzgas, and I. Gazaryan, Analytica. Chimica. Acta. 400 (1999) 91.

[5] S. Shleev, J. Tkac, A. Christenson, T. Ruzgas, A. I.Yaropolov, J. W. Whittaker, and L. Gorton, Biosens. Bioelectron. 20 (2005) 2517

[6] H. B. Gray, J. R. Winkler, Proc. Natl. Acad. Sci.USA 102 (2005) 3534.

[7] J.J. Kulys, AS. Samalius, Bioelectrochem. Biornerg. 13 (1984) 163.

[8] C. Léger, A. K. Jones, S. P. J. Albracht, and F. A. Armstrong, J. Phys. Chem. B. 106 (2002) 13058.

[9] R. A. Marcus, and N. Sutin, Biochimica. et. Biophysica. Acta. 811 (1985) 265.

[10] T. Ikeda, Direct redox communication between enzymes and electrodes, in: F. W. Scheller, F. Schubert, J. Fedrowitz (Eds.), Frontiers in Biosensorics I, Birkhäuser

[11] M. Ameyama, E. Shinagawa, K. Matsushita, and O. Adachi, J Bacteriol. 145 (1981) 814.

[12] K. Nakashima, H. Takei, O. Adachi, E. Shinagawa, and M. Ameyama, Clin. Chim. Acta.151 (1985) 307.

[13] R. Antiochia, and L. Gorton, Sens. Actuators B 195 (2014) 287.

[14] Y. Kamitaka, S. Tsujimura, and K. Kano, Chem. Lett. 36 (2007) 218.

[15] M. Tominaga, C. Shirakihara, and I. Taniguhi, J. Electroanal. Chem. 610 (2007) 1.

[16] T. Miyake, S. Yoshino, T. Yamada, K. Hata, and M. Nishizawa, J. Am. Chem. Soc. 133 (2011) 5129.

[17] J. Tkac, J. Svitel, I. Vostiar, M. Navratil, P. Gemeiner, Bioelectrochemistry 76 (2009) 53

Chapter 1

Heterologous Overexpression of a Flavoprotein-Cytochrome *c* Complex Fructose Dehydrogenase of *Gluconobacter japonicus* NBRC3260

For the first step in elucidation of the mechanism of DET-type bioelectrocatalytic reaction of FDH, the author tried to construct heterologous overexpression of *fdhSCL*. The *fdhSCL* genes encoding the FDH complex of *G. japonicus* NBRC3260 were isolated by a PCR-based gene amplification method with degenerate primers designed from the amino terminal amino acid sequence of the large subunit and sequenced. Three open reading frames for *fdhSCL* encoding the small, cytochrome c, and large subunits, respectively, were found and presumably in a polycistronic transcriptional unit. The expression system was conducted using a broad host range plasmid vector pBBR1MCS-4 carrying a DNA fragment containing the putative promoter region of the membrane-bound alcohol dehydrogenase gene of *Gluconobacter oxydans* and a *G. oxydans* strain as the expression host. The author also constructed a derivative modified in the translational initiation codon to ATG from TTG, designated as $_{TTG}$FDH and $_{ATG}$FDH. Membranes of the cells producing recombinant $_{TTG}$FDH and $_{ATG}$FDH showed approximately 20-times and 100-times higher specific activity than those of *G. japonicus* NBRC3260, respectively.

Introduction

Fructose dehydrogenase (FDH; EC 1.1.99.11) of *Gluconobacter japonicus* NBRC3260 (formerly *Gluconobacter industrius* IFO3260), which catalyzes the oxidation of D-fructose to produce 5-keto-D-fructose, is a heterotrimeric membrane-bound enzyme with a molecular mass of *ca.* 140 kDa, consisting of subunits I (67 kDa), II (51 kDa), and III (20 kDa). The enzyme, purified for the first time in 1981, is a flavoprotein-cytochrome *c* complex, since subunits I and II have covalently bound flavin adenine dinucleotide (FAD) and heme C as prosthetic groups, respectively [1]. FDH shows strict substrate specificity to D-fructose and thus is used in diagnosis and food analysis and is commercially available [2]. This enzyme is also used in a number of basic research projects to examine the electrochemical properties of enzyme-catalyzed electrode reactions, which is called bioelectrocatalysis [3]. The reaction is classified into two types. One is the direct

electron transfer (DET)-type system, in which electrons are transferred directly between the enzyme and electrode. The other is the mediated electron transfer (MET)-type system, in which mediators transfer electrons between the enzyme and electrode. As far as the author knows, FDH has the highest ability of DET-type bioelectrocatalysis on the anode [4]. The DET-type system is convenient for the construction of compact bioelectrochemical devices and is utilized to develop biosensors, biofuel cells, and bioreactors. However, DET-type bioelectrocatalysis occurs only at some limited kinds of electrodes suitable for individual redox enzymes, such as FDH [3], alcohol dehydrogenase [5], cellobiose dehydrogenase [6], bilirubin oxidase [7], and Cu efflux oxidase [8]. Although DET-type bioelectrocatalysis is attractive for applications, mechanisms for the reaction have not been fully described yet. For the first step to explore the mechanisms of the DET-type bioelectrocatalytic reaction of FDH, the author sequenced the genes encoding each subunit of the FDH complex from *G. japonicus* NBRC3260 and constructed an expression system to highly produce FDH in a *Gluconobacter oxydans* strain.

Experimental

Chemicals

Fructose dehydrogenase of *Gluconobacter japonicus* NBRC3260 was both a gift from and purchased from Toyobo (Osaka, Japan). Restriction endonucleases and modification enzymes for genetic engineering were kind gifts from Toyobo (Osaka, Japan) and were also purchased from TaKaRa Shuzo (Kyoto, Japan) and Agilent Technologies (Santa Clara, CA). Yeast extract was a generous gift from Oriental Yeast (Osaka, Japan). All other materials were purchased from commercial sources and were of a guaranteed grade.

Bacterial strains, plasmids, and growth conditions

The bacterial strains and plasmids used in this study are listed in Table 1. *Gluconobacter japonicus* NBRC3260 and *Gluconobacter oxydans* ATCC 621H and NBRC12528 and its Δ*adhA*::Km^R derivative [9] were used in this study. The broad-host-range vector pBBR1MCS-4 was used for the heterologous expression of the *fdhSCL* genes in *G. oxydans*. *Gluconobacter* spp. were grown on ΔP medium, consisting of 5 g of glucose, 20 g of glycerol, 10 g of polypeptone, and 10 g of yeast extract per liter, at 30 °C with vigorous shaking, unless otherwise stated. Kanamycin and ampicillin were used at final concentrations of 50 μg ml^{-1} and 250

μg ml^{-1}, respectively.

Escherichia coli DH5α was used for plasmid construction [10]. *E. coli* HB101 harboring pRK2013 was used as a helper strain for conjugative plasmid transfer, using a triparental mating method [11]. *E. coli* strains were grown on modified Luria-Bertani medium, consisting of 10 g of polypeptone, 5 g of yeast extract, and 5 g of NaCl, filled to 1 liter with distilled water and with the pH adjusted to 7.0 with NaOH. Ampicillin was used at a final concentration of 50 μg ml^{-1}.

Table 1. The bacterial strains and plasmids used in this study.

Strains and plasmids	Description	Source or reference
Bacterial strains		
Escherichia coli		
DH5α	F^- *endA1 hsdRJ7* (r_k^-, m_k^+) *supE44 thi-1* λ^- *recA1 gyrA96 relA1 deoR* Δ(*lacZYA-argF*)U169 ϕ80d*lacZ*ΔM15	[10]
HB101	F^- *thi-1 hsdS20* (r_B, m_B) *supE44 recA13 ara14 leuB6 proA2 lacY1 galK2 rpsL20* (str^r *xyl-5 mtl-1* λ^-)	[28]
Gluconobacter japonicas NBRC3260	Wild type	NBRC[a]
Gluconobacter oxydans		
NBRC12528	Wild type	NBRC[a]
Δ*adhA*	NBRC12528 Δ*adhA*::Km^R	[9]
ATCC621H	Wild type	ATCC[a]
Plasmids		
pKR2013	The plasmid mediates plasmid transfer, Km^R	[11]
pBBR1MCS-4	A broad host range plasmid, *mob* Ap^R	[29]
pSHO8	pBBR1MCS-4, a 0.7-kb fragment of a putative promoter region of the *adhAB* gene of *G. oxydans* 621H	This study
pSHO12	pSHO8, a 3.8-kb fragment of the *fdhSCL* genes of *G. japonicus* NBRC3260	This study

pSHO13	pSHO8, a 3.7-kb fragment of the *fdh*$_{ATG}$*SCL* genes	This study
pSHO16	pSHO8, a 2.4-kb fragment of the *fdh*$_{ATG}$*SL* genes (in-frame deletion of *fdhC*)	This study

[a], The URL addresses of NBRC and ATCC are "http://www.nbrc.nite.go.jp/" and "http://www.atcc.org/", respectively.

Determination of the N-terminal amino acid sequence of purified FDH

Commercially available FDH was subjected to SDS-PAGE (10% acrylamide). The proteins in the gel were transferred electrophoretically onto a polyvinylidene difluoride membrane at 2 mA cm^{-2} for 40 min. Proteins were stained with CBB (Coomassie brilliant blue) stain one (Nacalai Tesque, Japan), destained with 5% (vol vol^{-1}) methanol, followed by the excision and drying of bands. The N-terminal amino acid sequence was analyzed with the peptide sequencer Procise 491 (Life Technologies, Carlsbad, CA, USA).

Sequencing of the fdhSCL genes

Degenerate primers, Forward primer A and Reverse primer B, were designed for PCR-based gene amplification (Table S1). The genomic DNA of *G. japonicus* was isolated from cells grown to a mid-exponential phase of growth by the method of Marmur [12] with some modifications, *i.e.* the author used cetyltrimethylammonium bromide at a final concentration of 1% (wt vol^{-1}) to remove polysaccharides but omitted the perchlorate step in the original procedure. PCR was performed with the genomic DNA of *G. japonicus* as the parental DNA molecule using KOD Dash polymerase (Toyobo, Japan) and the MyCycler thermal cycler (Bio-Rad, CA, USA). The amplified DNA fragment was sequenced using the same primers. The thermal asymmetric interlaced PCR (TAIL-PCR) method was repeatedly conducted to extend sequencing to the 5' and 3' directions using one of the three arbitrary degenerate primers, AD1, AD2, or AD3, and KOD Dash polymerase, according to Liu *et al.* [13]. The product of TAIL-PCR was sequenced to be homologous to the 3' region of the gene encoding the cytochrome *c* subunit of sorbitol dehydrogenase. Thus, degenerate primers were designed from the conserved amino acid sequence in the heme C binding motives in the cytochrome *c* subunits of other dehydrogenases to extend sequencing. The author repeated the TAIL-PCR method to further obtain the complete structural genes for the FDH

complex.

Construction of plasmids

For plasmid construction, the auhtor used Herculase II Fusion DNA polymerase (Agilent Technologies, Santa Clara, CA, USA) to amplify the designed DNA fragments. A putative promoter region of the *adhAB* genes, which encode two major subunits of the pyrroloquinoline quinone-dependent alcohol dehydrogenase, was amplified with Herculase II Fusion DNA polymerase using a genomic DNA preparation of *G. oxydans* 621H and two primers, 621H-adh-pro(+) and 621H-adh-pro(-) (Table S1). The PCR product was inserted into pBBR1MCS-4 [9] treated with *Kpn*I and *Xho*I to yield pSHO8. The *fdhSCL* genes were amplified with the DNA polymerase using the genome DNA of *G. japonicus* NBRC3260 and two primer sets, fdhS-5-Eco(+) and fdhL-3-PstBam(-) and fdhS-370-ATG-Xho(+) and fdhL-3-PstBam(-) (Table S1), respectively. The PCR products were inserted into pSHO8 treated with *Eco*RI and *Bam*HI and with *Xho*I and *Bam*HI to yield pSHO12 and pSHO13, respectively. To construct a plasmid to express only the *fdhSL* genes, an in-frame deletion in the *fdhC* gene was introduced in pSHO13 by fusion PCR as follows. The 5' and 3' fragments for a deletion derivative of pSHO13, in which most of subunit II (from His^{11} to Trp^{451}, amino acid number of the putative mature subunit II) is lost in-frame, were amplified with the DNA polymerase with the primer sets of fdhS-370-ATG-Xho(+) and delta-fdhC(-) and delta-fdhC(+) and fdhL-3-PstBam(-), respectively (Table S1). The two PCR products were purified and conducted to fusion PCR with the primers fdhS-370-ATG-Xho(+) and fdhL-3-PstBam(-). The amplified 2.4-kb DNA fragment was inserted into pSHO8 treated with *Xho*I and *Bam*HI to yield pSHO16. All nucleotide sequences of PCR cloning were confirmed by cycle sequencing techniques using a 310 DNA sequencer (Applied Biosystems, CA, USA).

Expression of recombinant FDH and preparation of the membrane fraction

G. oxydans NBRC12528 Δ*adhA*::Km^R was transformed with the plasmids via a triparental mating method using the HB101 strain harboring pRK2013 [11]. Acetic acid was added to the media for selection at a final concentration of 0.1% (wt vol^{-1}) to eliminate *E. coli* growth. Acetic acid- and ampicillin-resistant conjugant colonies were screened twice on ΔP agar medium containing 0.1% (wt vol^{-1}) acetic acid and 250 μg ml^{-1} ampicillin. Finally, the transconjugants were screened in liquid ΔP medium containing 250 μg ml^{-1} ampicillin.

Gluconobacter cells were cultivated in ΔP medium with or without 250 μg ml^{-1} ampicillin to the late exponential growth phase. Cells were collected by

centrifugation at 10,000×*g* for 10 min and washed twice with 20-fold-diluted McIlvaine buffer (pH 6.0). Preparation of the membrane fraction was carried out as described by Ameyama *et al.* [1] with some modifications, as follows. Cells were suspended in 20-fold-diluted McIlvaine buffer (pH 6.0) and were disrupted by two passages through a French pressure cell press (Thermo Fisher Scientific, Waltham, MA, USA). After cell debris was sedimented by low speed centrifugation (10,000×*g*, 10 min, 4 °C), the supernatant was ultracentrifuged (100,000×*g*, 1 h, 4 °C). The supernatant was used as the soluble fraction and precipitates were resuspended in 20-fold-diluted McIlvaine buffer (pH 6.0) and used as the membrane fraction.

Purification of recombinant FDH

The solubilization and purification of FDH were performed as described [1] with some modifications, as follows. Membranes were suspended in 20-fold diluted McIlvaine buffer (pH 6.0) at a concentration of 10 mg membrane protein ml^{-1} containing 1 mM 2-mercaptoethanol and 1.0% (wt vol^{-1}) Triton X-100 and gently stirred for 10 h at 4 °C. FDH was obtained in the supernatant fraction of ultracentrifugation at 100,000×g for 1.5 h. The supernatant fraction was applied on a DEAE-Sepharose column equilibrated with 20-fold diluted McIlvaine buffer (pH 6.0) containing 1 mM 2-mercaptoethanol and 0.1% (wt vol^{-1}) Triton X-100. The elution of FDH from a DEAE-Sepharose column was carried out by a concentration gradient of McIlvaine buffer, i.e. from 20-fold diluted McIlvaine buffer (pH 6.0) to the original concentrations of McIlvaine buffer (pH 6.0) containing 1 mM 2-mercaptoethanol and 0.1% (wt vol^{-1}) Triton X-100. The purities of recombinant FDH were judged by Coomassie brilliant blue R-250 staining of SDS-PAGE.

Oxygen consumption rates by intact cells

Oxygen consumption of intact *Gluconobacter* cells was measured at 25 °C with a Clark-type oxygen electrode (OPTO SCIENCE, Tokyo, Japan). Cell suspensions were prepared at concentrations of 1.0 OD_{600nm} with 50 mM sodium phosphate buffer (pH 6.0). D-Glucose and D-fructose were added at 200 mM as the respiration substrate. Oxygen concentrations were recorded amperometrically as the reduction current of oxygen at -600 mV vs. the Ag|AgCl reference electrode.

Other analytical methods

Global identity between predicted amino acid sequences was calculated by the software GENETYX-MAC (ver. 14; GENETYX, Tokyo, Japan). Protein

concentrations were determined with the DC Protein Assay Kit (Bio-Rad, CA, USA) using bovine serum albumin as a standard. FDH activity was measured spectrophotometrically with potassium ferricyanide and the ferric-dupanol reagent as described [1]. One FDH unit was defined as the enzyme amount oxidizing one micromole of D-fructose per min. Covalently bound heme C on protein separated by SDS-PAGE was stained by heme-catalyzed peroxidase activity [14]. Heme C content was determined spectrophotometrically as described [15].

Nucleotide sequence accession number

The nucleotide sequence and their predicted amino acid sequence were deposited to the DNA data bank of Japan (DDBJ) with the accession number of AB728565.

Results and discussion

Sequencing of the fdhSCL genes

The author determined the N-terminal amino acid sequence of subunit I of the commercially available FDH complex purified from *G. japonicus* NBRC3260 (*Gluconobacter* sp. in the instructions provided by Toyobo) to be SNETLSADVVIIGAGICGSLLAH (in an amino to carboxyl direction) as shown in Fig. S1. Basic Local Alignment Search Tool (BLAST) analysis of the determined amino acid sequence revealed that subunit I of sorbitol dehydrogenase (SLDH) of *Gluconobacter frateurii* THD32 shows the highest identity with the N-terminal amino acid sequence of subunit I of FDH [16]. The author thus designed degenerate primers for PCR (Table S1) based on the N-terminal sequence and conserved the amino acid sequence in the SLDH subunit I, respectively. To obtain sequence information upstream and downstream of the PCR product, the TAIL-PCR method was conducted as described in the Materials and Methods section. The Author also designed degenerate primers from the heme C binding consensus sequence, and further repeated the TAIL-PCR method. The author determined the nucleotide sequence of the 4,208-base PCR product containing the complete structural genes for the FDH complex.

The nucleotide and predicted amino acid sequences of FDH and the flanking regions are shown in Fig. S1. Three open reading frames (ORFs) were found for *fdhSCL* encoding the small, cytochrome *c,* and large subunits, or subunit III, II, and I, respectively. They may be in the same transcriptional unit. A sequence of

SRRKLLA, similar to the consensus motif SRRXFLK (where X is any polar amino acid) for the twin-arginine translocation (tat) system of *E. coli* that translocates secretory proteins across the cytoplasmic membrane, was found in the N terminus of FdhS [17]. Since there was no ATG or GTG codon between the tat signal and nonsense codon in the upstream region, a TTG codon at nucleotide (nt) 93 can be the start codon for *fdhS*. A possible Shine-Dalgarno sequence was found at 6-bp upstream of this start codon. The author did not find a rho-independent terminator-like sequence around the termination codon for *fdhL*, rather there seems to have been another ORF from nt 3,794 of which the product is homologous to the hypothetical protein GDI_0857 of *Gluconacetobacter diazotrophicus* PAI5 and the hypothetical protein GMO_23960 of *Gluconobacter morbifer* G707. Since the author failed to obtain the sequence for upstream and downstream regions of the *fdhSCL* genes, a whole structure of the *fdh* operon is uncertain. A 35-amino acid stretch in the predicted N terminus of subunit III can be recognized as a signal sequence by the SOSUIsignal program [18], whereas no signal sequence was found for the N terminus of subunit I, suggesting that subunit I may be translocated together with subunit III by the tat system. The *fdhS* gene encoded 183 amino acids but 148 for the mature protein, of which the calculated molecular mass was approx. 16 kDa.

The ORF corresponding to subunit II, *fdhC*, started at the position of nt 663. A possible SD sequence, AGGA, was found 15-nt upstream of the start codon. The 25 amino acid sequence of the predicted N terminus of FdhC was suggested as a sec-dependent signal sequence by the SOSUIsignal program [18]. The molecular mass of the mature protein could be calculated as approx. 49 kDa composed of 461 amino acids, but it should be higher because the deduced amino acid sequence was revealed to have three CXXCH sequence motives for heme C binding sites.

The coding region of subunit I was started at position 2,145 with the ATG codon. There was a possible SD sequence, AGG, 9-nt upstream of the initiation codon. No signal sequence for translocation was found in the predicted sequence, consistent with the result of the N-terminal amino acid sequencing of purified FDH, which started at the second Ser residue. The *fdhL* gene encoded a polypeptide of 544 amino acid residues with a calculated molecular mass of approx. 60 kDa being assembled with and covalently bound to FAD. The deduced amino acid sequence was found to have the GAGICG sequence at a position between the 14th and 19th residues, corresponding to the binding motif of FAD (GXGXXG) [19].

Global identity between the predicted amino acid sequences of each subunit of FDH and SLDH from *G. frateurii* [16] was calculated as follows using the putative

mature forms of protein: subunit I, 52% identity; subunit II, 44% identity; subunit III, 24% identity. Even though there are high identities, the SLDH of *Gluconobacter thailandicus* NBRC3254 (formally *Gluconobacter suboxydans* subsp. α IFO3254) closely related to that of *G. frateurii* [16] has been shown to be inert on sugars but active on D-mannitol at only a 5% rate of D-sorbitol [20]. The global identity of each subunit of FDH with that of GDH from *Burkholderia cepacia* [21] was 52%, 45%, and 32% for subunit I, subunit II, and subunit III, respectively. *B. cepacia* GDH shows relatively wide substrate specificity, *i.e.* this enzyme oxidizes maltose at half the rate of D-glucose [22]. On the other hand, since thorough substrate specificity has not been reported so far, it is not clear yet whether *B. cepacia* GDH oxidizes other monosaccharides.

The putative mature form of the predicted amino acid sequence of *fdhC* showed considerable identity to those of the cytochrome *c* subunits of ADH of *G. oxydans* (36%, [23]) and aldehyde dehydrogenase of *Gluconacetobacter europaeus* (31%, [24]).

Construction of Gluconobacter strains for fdhSCL expression

Since *G. oxydans* NBRC12528 highly produces *c*-type cytochromes and flavoproteins [25] but does not have FDH activity [1], the author tried heterologous expression of the *fdhSCL* genes in this strain. Moreover, because ADH is one of major membrane proteins in NBRC12528 and may disturb protein purification, its derivative, which has gene replacement in the *adhA* gene encoding a large subunit of ADH (Δ*adhA*::Km^R strain), was used in this study. The broad-host-range plasmid vector pBBR1MCS-4 was stable in *G. oxydans* NBRC12528 and easy to manipulate, thus the author used this plasmid vector to express the *fdhSCL* genes. To ensure heterologous expression, a putative promoter region for the *adhAB* genes of *G. oxydans* 621H was inserted at the upstream region of the *fdhSCL* genes.

Judging from the multiple alignment analysis of subunit III of several flavoprotein-cytochrome *c* complex dehydrogenases (data not shown), the start codon of the FdhS subunit seemed to be TTG and not ATG. In addition to simple cloning of the native *fdhSCL* genes, in order to confirm the translational start site of subunit III and examine translation efficiency, we constructed modified *fdhSCL* genes to designate $fdh_{ATG}SCL$, where the TTG codon was replaced with ATG and a termination codon (TAA) was inserted just before the ATG codon. The Δ*adhA* strain was transformed with the constructed plasmids by conjugation-based gene transfer.

Comparison between wild-type and recombinant FDHs

The *G. japonicus* NBRC3260 strain, which produces wild-type FDH, showed 0.15 FDH units (mg membrane protein)$^{-1}$ in the membranes. Although the author did not examine this in detail, the low specific FDH activity in the membranes of *G. japonicus* NBRC3260 may be attributed to the difference in the media used in the present and former studies, *i.e.* ΔP medium was used in this study, while the former study used synthetic medium. Membranes of the Δ*adhA* cells harboring pSHO12 carrying the wild-type *fdhSCL* genes showed 3.5 ± 0.3 units mg^{-1}, activity approximately 20-times higher than those of *G. japonicus* NBRC3260 (Fig. 1). Furthermore, those of $_{ATG}$FDH showed 16 ± 0.8 units mg^{-1}, approximately 5-times higher than $_{TTG}$FDH. We could not detect FDH activity in the membranes of the Δ*adh* strain harboring pSHO8 carrying the putative promoter region only.

Heme-catalyzed peroxidase staining of the SDS-PAGE gel revealed that both membranes having $_{TTG}$FDH and $_{ATG}$FDH showed approx. 51-kDa bands, while the Δ*adh* strain harboring pSHO8 did not. The apparent intensity of staining of $_{ATG}$FDH was the highest in the samples examined in this study, and that of $_{TTG}$FDH was also higher than that of *G. japonicus* NBRC3260 (data not shown). These results clearly indicate that the initiation codon for subunit III is TTG at nt 93, and also suggest that expressions of not only subunit III, but also the whole FDH complex are increased by changing the initiation codon to ATG.

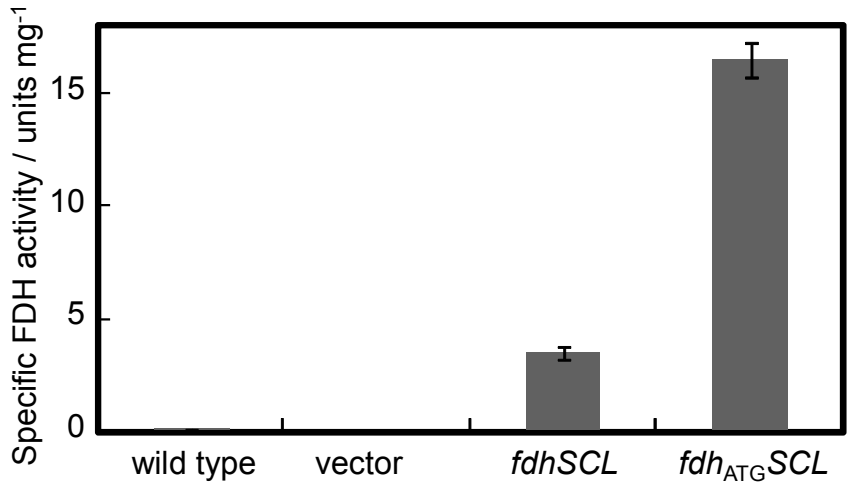

Figure 1. Comparison of specific FDH activity in the membranes of *G. japonicus* NBRC3260 (wild type) and the Δ*adh* strains harboring pSHO8 (vector), pSHO12 (native *fdhSCL*), or pSHO13 ($fdh_{ATG}SCL$). Data are shown as mean values with 90% confidence intervals (error bars; $n = 3$).

Characterization of purified ATGFDH

The specific activity of ATGFDH purified in this study was 260 units (mg protein)$^{-1}$ at 25 °C, which is approx. 1.5-times higher than that reported in the previous study [1]. The purified ATGFDH had three main bands of 68, 51, and 18 kDa on SDS-PAGE (Fig. 2), which are similar sizes to those reported previously [1], and correspond with the expected molecular masses from the *fdhSCL* genes determined in this study. At least two smaller bands could be seen in the CBB-stained SDS-PAGE of our FDH preparation (Fig. 2). However, the author did not find these bands when we used other detergents for preliminary FDH purification, such as *n*-dodecyl-β-D-maltoside and *n*-octyl-β-D-glucoside (data not shown). Thus, the author likely considers them as contaminants.

The purified ATGFDH showed a reduced cytochrome *c*-like absorption spectrum (data not shown), which is derived from the heme C moieties in subunit II. Based on the FDH complex being a heterotrimeric structure, the number of heme C was determined to be 2.1 per complex, which was calculated from spectrometric heme C contents and protein contents as described in the Experimental section. The author suggests that FDH has three heme C moieties as predicted from the deduced amino acid sequence of subunit II, although the estimated value is more than two but much less than three, because some protein impurities can be seen in the

CBB-stained SDS-PAGE of our FDH preparation (Fig. 2) and minor invisible contaminations are also possible.

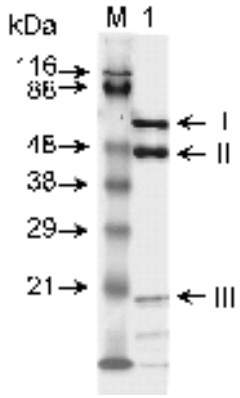

Figure 2. Coomassie staining of the purified FDH complex separated by SDS-PAGE. Lane M, Molecular mass standard and 10 μg of the purified FDH complex were applied on lanes 1 and M, respectively.

Characterization of the subunit I/III subcomplex

To examine the roles of subunit II in the electron transfer to ubiquinone, the physiological electron acceptor, and ferricyanide, an artificial electron acceptor, and in the subcellular localization of the FDH complex, the author constructed a strain to produce only subunits I and III. Oxygen consumption with D-glucose and D-fructose by the Δ*adhA* cells harboring pSHO8 (vector), pSHO13 (*fdh*$_{ATG}$*SCL*), or pSHO16 (*fdh*$_{ATG}$*SL*) were measured (Fig. 3). D-Fructose-dependent oxygen consumption by the Δ*adhA* cells harboring the empty vector was much lower than oxygen consumption with glucose by the same cells ($p < 0.01$, Student's t test; $n = 6$), suggesting that the Δ*adhA* strain and even the parental strain *G. oxydans* NBRC12528 have the glucose oxidizing respiratory chain as previously reported [26], but do not have the fructose oxidizing respiratory chain. They presumably have the ability to metabolize D-fructose to produce NADH being re-oxidized by the respiratory chain. D-Glucose-dependent oxygen consumption rates by the Δ*adhA* cells harboring pSHO13 (*fdh*$_{ATG}$*SCL*) and pSHO16 (*fdh*$_{ATG}$*SL*) were increased by approx. 1.5-fold that of the cells harboring pSHO8 (vector) by a mechanism that has yet to be elucidated ($p < 0.01$, Student's t test; $n = 6$). The cells harboring pSHO13 (*fdh*$_{ATG}$*SCL*) showed the ability to consume oxygen depending on fructose at approx. a 10-fold faster rate than that of the cells harboring the empty vector ($p < 0.01$, Student's t test; $n = 6$), which is much higher than that observed with glucose,

suggesting that the fructose-oxidizing respiratory chain was heterologously reconstituted in the Δ*adhA* cells. On the other hand, the difference in D-fructose-dependent oxygen consumption between the cells harboring pSHO16 (*fdh*$_{ATG}$*SL*) and those harboring the empty vector may be considered negligible ($p > 0.1$, Student's t test; $n = 6$).

In order to know whether the functional subunit I/III subcomplex is expressed, the author examined the *in vitro* fructose dehydrogenase activity of the cell-free extract of the Δ*adhA* cells harboring pSHO16 (*fdh*$_{ATG}$*SL*). The activity of the cells that express whole FDH complex could be found mostly in the membrane fraction at a specific activity of 20 ± 5 units mg^{-1} at pH 5.0 (Fig. 4A). However, the activity of the cells that express the subunit I/III subcomplex (FdhSL) was detected mostly in the soluble fraction at a specific activity of 3.8 ± 0.4 units mg^{-1}, indicating that functional FdhSL is produced and subunit II is a membrane-anchoring subunit for the FDH complex. Because FdhSL had significant activity to oxidize fructose but failed to link the respiratory chain, it is reasonable to conclude that subunit II is responsible for ubiquinone reduction. The author examined the pH-dependency of fructose dehydrogenase activity for the FDH complex in the membrane fraction and FdhSL in the soluble fraction (Fig. 4B). They were different from each other, i.e. the optimum pH of the FDH complex in the membrane fraction was pH 4.0, whereas FdhSL showed the highest activity at pH 6.0.

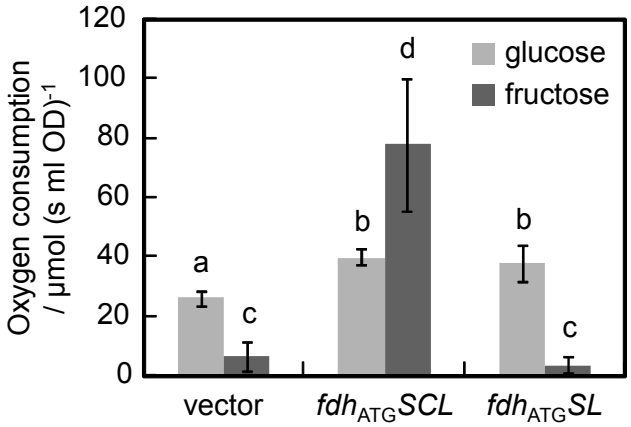

Figure 3. D-Fructose-dependent oxygen consumption (heavy gray columns) of the whole cell preparations of the Δ*adh* strains harboring either pSHO8 (vector), pSHO13 ($fdh_{ATG}SCL$), or pSHO16 ($fdh_{ATG}SL$). Control experiments were also conducted with D-glucose (light gray columns). The rates of oxygen consumption were normalized by optical density of the cell preparations. Data are shown as mean values with 90% confidence intervals (error bars; $n = 3$). Significance can be seen between columns with a and b, a and c, and c and d ($p < 0.01$, Student's t test; $n = 6$). Columns with the same letters were not significantly different ($p > 0.1$, Student's t test; $n = 6$).

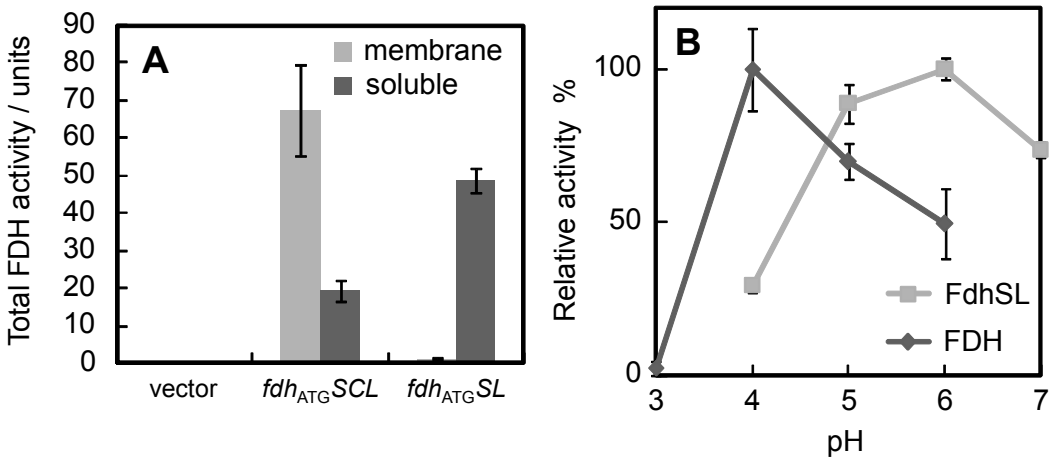

Figure 4. Comparison of the FDH complex (FDH) and I/III. (A) The membrane (light gray columns) and soluble (heavy gray columns) fractions of the Δ*adhA* strains harboring pSHO8 (vector), pSHO13 ($fdh_{ATG}SCL$), or pSHO16 ($fdh_{ATG}SL$) were prepared, and FDH activity in the membrane and soluble fractions were measured at pH 5.0 and pH 6.0, respectively. Total activity in each fraction was shown. (B) FDH activities of the membrane fraction for the FDH complex (heavy gray diamonds) and the soluble fraction for FdhSL (light gray squares) were measured under various pH conditions. Relative activity to that of the highest activity was shown individually. Data are shown as mean values with 90% confidence intervals (error bars; $n = 3$). The specific FDH activities of the membrane fraction of the cells harboring pSHO13 ($fdh_{ATG}SCL$) and the soluble fraction of the cells harboring pSHO16 ($fdh_{ATG}SL$) were 20 ± 5 and 3.8 ± 0.4 units mg^{-1}, respectively.

References

[1] M. Ameyama, E. Shinagawa, K. Matsushita, and O. Adachi, J Bacteriol. 145 (1981) 814.

[2] K. Nakashima, H. Takei, O. Adachi, E. Shinagawa, and M. Ameyama, Clin. Chim. Acta.151 (1985) 307.

[3] Y. Kamitaka, S. Tsujimura, and K. Kano, Chem. Lett. 36 (2007) 218.

[4] Y. Kamitaka, S. Tsujimura, N. Setoyama, T. Kajino, and K. Kano, Phys. Chem. Chem. Phys. 9 (2007) 1793.

[5] T. Ikeda, D. Kobayashi, F. Matsushita, T. Sagara, and K. Niki, Journal of Electroanalytical Chemistry. 361 (1993) 221.

[6] L. Gorton L, A. Lindgren, T. Larsson, F. D. Munteanu, T. Ruzgas, and I. Gazaryan, Analytica. Chimica. Acta. 400 (1999) 91.

[7] S. Tsujimura, T. Nakagawa, K. Kano, and T. Ikeda, Electrochemistry . 72 (2004) 437.

[8] Y. Miura, S. Tsujimura, Y. Kamitaka, S. Kurose, K. Kataoka, T. Sakurai, and K. Kano K, Chem. Lett. 36 (2007) 132.

[9] H. Habe, Y. Shimada, T. Yakushi, H. Hattori, Y. Ano, T. Fukuoka, D. Kitamoto, M. Itagaki, K. Watanabe, H. Yanagishita, K. Matsushita, and K. Sakaki, Appl. Environ. Microbiol. 75 (2009) 7760.

[10] S. G. Grant, J. Jessee, F. R. Bloom, and D. Hanahan, Proc. Natl. Acad. Sci. U S A. 87 (1990) 4645.

[11] D. H. Figurski, D. R. Helinski, Proc. Natl. Acad. Sci. U S A. 76 (1979) 1648.

[12] J. Marmur, Methods in Enzymology. 6 (1963) 726.

[13] Y. G. Liu, N. Mitsukawa, T. Oosumi, and R. F. Whittier, Plant. J. 8 (1995) 457.

[14] C. F. Goodhew, K. R. Brown, and G. W. Pettigrew, Biochimi. Biophys. Acta. 852 (1986) 288.

[15] E. A. Berry, and B. L. Trumpower, Anal. Biochem. 161 (1987) 1.

[16] H. Toyama, W. Soemphol, D. Moonmangmee, O. Adachi, and K. Matsushita, Biosci. Biotechnol. Biochem. 69 (2005) 1120.

[17] B. C. Berks, T. Palmer, and F. Sargent, Curr. Opin. Microbiol. 8 (2005) 174.

[18] M. Gomi, M. Sonoyama, and S. Mitaku, Chem-Bio Informatics Journal. 4 (2004) 142.

[19] O. Dym, and D. Eisenberg, Protein. Sci. 10 (2001) 1712.

[20] E. Shinagawa, K. Matsushita, O. Adachi, and M. Ameyama, Agric. Biol. Chem. 46 (1982) 135.

[21] T. Tsuya, S. Ferri, M. Fujikawa, H. Yamaoka, and K. Sode, J. Biotechnol. 123 (2006) 127.

[22] H. Yamaoka, Y. Yamashita, S. Ferri, and K. Sode, Biotechnol. Lett. 30 (2008) 1967.

[23] K. Kondo, and S. Horinouchi, Appl. Environ. Microbiol.63 (1997) 1131.

[24] C. Thurner, C. Vela, L. Thony-Meyer, L. Meile, and M. Teuber, Arch. Microbiol. 168 (1997) 81.

[25] K. Matsushita, H. Toyama, and O. Adachi, Adv. Microb. Physiol. 36 (1994) 247.

[26] K. Matsushita, E. Shinagawa, O. Adachi, and M. Ameyama, J. Biochem. 105 (1989) 633.

[27] S. Kawai, T. Yakushi, K. Matsushita, Y. Kitazumi, O. Shirai, and K. Kano, Electrochem. Commun. 38 (2014) 28.

[28] H. W. Boyer, and D. Roulland-Dussoix, J. Mol. Biol. 41 (1969) 459.

[29] M.E. Kovach, P. H. Elzer, D. S. Hill, G. T. Robertson, M. A. Farris, R. M. Roop 2nd, and K. M. Peterson, Gene. 166 (1995) 175.

Table S1. Oligonucleotides used in this study.

Primer name	Sequence (5′ --> 3′)[a]	Objective
Forward primer A	CSGCCGAYGTCGTGATYATYGGTG	Degenerate PCR and sequencing
Reverse primer B	GGCARATCGGCATRCARTTRTTRTTNCC	Degenerate PCR and sequencing
AD1	NTCGASTWTSGWGTT	TAIL-PCR
AD2	NGTCGASWGANAWGAA	TAIL-PCR
AD3	WGTGNAGWANCANAGA	TAIL-PCR
621H-adh-pro(+)	GGGGTACCTTCTGGCGGTACGGAGTC[b]	pSHO8
621H-adh-pro(-)	CCGCTCGAGATTAACCAGAAGTCATGATCCAAC[b]	pSHO8
fdhS-5-Eco(+)	GAATTCCAAACAAAAAATAGTC[b]	pSHO12
fdhL-3-PstBam(-)	GGATCCTGCAGCGTGGCGTTGAAACACTG[b]	pSHO12
fdhS-370-ATG-Xho(+)	CTCGAGGAGAAGGTAAATGGAAAAAATAGCTGATTC[b]	pSHO13
delta-fdhC(+)	gaaccaacacctgcttcagcgCTGATCAGCCGTCGCAAAAAG[c]	pSHO16
delta-fdhC(-)	CTTTTTGCGACGGCTGATCAGcgctgaagcaggtgttggttc[c]	pSHO16

[a], N = A, C, G, or T; R = A or G; Y = C or T.

[b], The engineered endonuclease recognition site is underlined.

[c], The 3' and 5' regions of *fdhC* are shown in lower and upper cases, respectively.

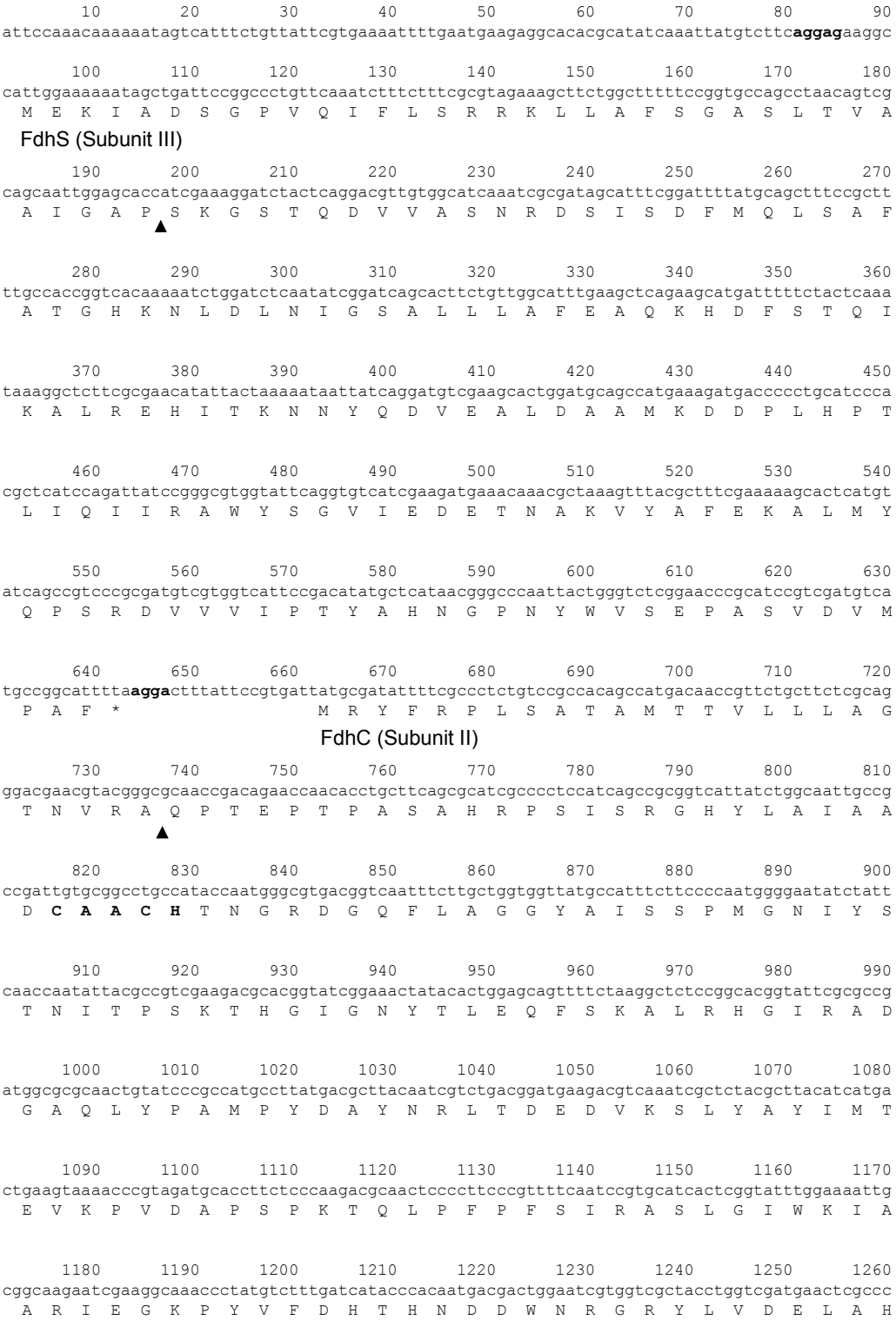
10 20 30 40 50 60 70 80 90
attccaaacaaaaaatagtcatttctgttattcgtgaaaattttgaatgaagaggcacacgcatatcaaattatgtcttcaggagaaggc
100 110 120 130 140 150 160 170 180
cattggaaaaaatagctgattccggccctgttcaaatctttctttcgcgtagaaagcttctggctttttccggtgccagcctaacagtcg
M E K I A D S G P V Q I F L S R R K L L A F S G A S L T V A
FdhS (Subunit III)
190 200 210 220 230 240 250 260 270
cagcaattggagcaccatcgaaaggatctactcaggacgttgtggcatcaaatcgcgatagcatttcggattttatgcagctttccgctt
A I G A P S K G S T Q D V V A S N R D S I S D F M Q L S A F
280 290 300 310 320 330 340 350 360
ttgccaccggtcacaaaaatctggatctcaatatcggatcagcacttctgttggcatttgaagctcagaagcatgatttttctactcaaa
A T G H K N L D L N I G S A L L L A F E A Q K H D F S T Q I
370 380 390 400 410 420 430 440 450
taaaggctcttcgcgaacatattactaaaaataattatcaggatgtcgaagcactggatgcagccatgaaagatgacccccctgcatccca
K A L R E H I T K N N Y Q D V E A L D A A M K D D P L H P T
460 470 480 490 500 510 520 530 540
cgctcatccagattatccgggcgtggtattcaggtgtcatcgaagatgaaacaaacgctaaagtttacgctttcgaaaaagcactcatgt
L I Q I I R A W Y S G V I E D E T N A K V Y A F E K A L M Y
550 560 570 580 590 600 610 620 630
atcagccgtcccgcgatgtcgtggtcattccgacatatgctcataacgggcccaattactgggtctcggaacccgcatccgtcgatgtca
Q P S R D V V V I P T Y A H N G P N Y W V S E P A S V D V M
640 650 660 670 680 690 700 710 720
tgccggcatttaaggactttattccgtgattatgcgatattttcgccctctgtccgccacagccatgacaaccgttctgcttctcgcag
P A F * M R Y F R P L S A T A M T T V L L L A G
FdhC (Subunit II)
730 740 750 760 770 780 790 800 810
ggacgaacgtacgggcgcaaccgacagaaccaacacctgcttcagcgcatcgcccctccatcagccgcggtcattatctggcaattgccg
T N V R A Q P T E P T P A S A H R P S I S R G H Y L A I A A
820 830 840 850 860 870 880 890 900
ccgattgtgcggcctgccataccaatgggcgtgacggtcaatttcttgctggtggttatgccatttcttccccaatggggaatatctatt
D C A A C H T N G R D G Q F L A G G Y A I S S P M G N I Y S
910 920 930 940 950 960 970 980 990
caaccaatattacgccgtcgaagacgcacggtatcggaaactatacactggagcagttttctaaggctctccggcacggtattcgcgccg
T N I T P S K T H G I G N Y T L E Q F S K A L R H G I R A D
1000 1010 1020 1030 1040 1050 1060 1070 1080
atggcgcgcaactgtatcccgccatgccttatgacgcttacaatcgtctgacggatgaagacgtcaaatcgctctacgcttacatcatga
G A Q L Y P A M P Y D A Y N R L T D E D V K S L Y A Y I M T
1090 1100 1110 1120 1130 1140 1150 1160 1170
ctgaagtaaaacccgtagatgcaccttctcccaagacgcaactccccttcccgttttcaatccgtgcatcactcggtatttggaaaattg
E V K P V D A P S P K T Q L P F P F S I R A S L G I W K I A
1180 1190 1200 1210 1220 1230 1240 1250 1260
cggcaagaatcgaaggcaaaccctatgtctttgatcatacccacaatgacgactggaatcgtggtcgctacctggtcgatgaactcgccc
A R I E G K P Y V F D H T H N D D W N R G R Y L V D E L A H

```
     1270      1280      1290      1300      1310      1320      1330      1340      1350
attgtggagagtgtcacacaccgcgtaactttcttctagcgcccaatcagtccgcttatcttgctggtgcggacataggatcatggcgtg
  C  G  E  C  H  T  P  R  N  F  L  L  A  P  N  Q  S  A  Y  L  A  G  A  D  I  G  S  W  R  A

     1360      1370      1380      1390      1400      1410      1420      1430      1440
caccaaatattaccaatgcccctcaaagcggtattggcagttggtcggatcaggatctcttccaatatctgaaaactggaaaaaccgcac
  P  N  I  T  N  A  P  Q  S  G  I  G  S  W  S  D  Q  D  L  F  Q  Y  L  K  T  G  K  T  A  H

     1450      1460      1470      1480      1490      1500      1510      1520      1530
atgctcgtgcagcaggaccaatggcagaagcaatcgagcatagcctacaatatcttccggatgccgatatttctgccatagttacatatc
  A  R  A  A  G  P  M  A  E  A  I  E  H  S  L  Q  Y  L  P  D  A  D  I  S  A  I  V  T  Y  L

     1540      1550      1560      1570      1580      1590      1600      1610      1620
ttcgttcggttccggcaaaggcagaaagcggtcaaacagtcgctaattttgagcatgccggccgcccatccagttacagtgttgctaacg
  R  S  V  P  A  K  A  E  S  G  Q  T  V  A  N  F  E  H  A  G  R  P  S  S  Y  S  V  A  N  A

     1630      1640      1650      1660      1670      1680      1690      1700      1710
ctaactcccgtcgcagcaatagtactctgacaaaaacaaccgatggtgctgcactctacgaggctgtgtgcgccagttgccatcaatctg
  N  S  R  R  S  N  S  T  L  T  K  T  T  D  G  A  A  L  Y  E  A  V  C  A  S  C  H  Q  S  D

     1720      1730      1740      1750      1760      1770      1780      1790      1800
acggtaaagggtccaaagacggttattatccttccctcgtaggaaatacgacgaccgggcaactcaatccaaatgatctgatcgccagta
  G  K  G  S  K  D  G  Y  Y  P  S  L  V  G  N  T  T  T  G  Q  L  N  P  N  D  L  I  A  S  I

     1810      1820      1830      1840      1850      1860      1870      1880      1890
ttctttacggtgtggaccgcacaacggataaccacgaaatcctgatgccggcttttggtccagactctctcgtacagcccctgacagatg
  L  Y  G  V  D  R  T  T  D  N  H  E  I  L  M  P  A  F  G  P  D  S  L  V  Q  P  L  T  D  E

     1900      1910      1920      1930      1940      1950      1960      1970      1980
agcagatcgccacaatcgcggactacgttctaagccactttggcaatgcccaggccacagtctcggcagatgcggtcaaacaggtgcggg
  Q  I  A  T  I  A  D  Y  V  L  S  H  F  G  N  A  Q  A  T  V  S  A  D  A  V  K  Q  V  R  A

     1990      2000      2010      2020      2030      2040      2050      2060      2070
cgggcggaaagcaggttcctctcgccaagctcgccagtccgggcgtgatgctgcttctcggaactggtggcatcctgggagccattctgg
  G  G  K  Q  V  P  L  A  K  L  A  S  P  G  V  M  L  L  L  G  T  G  G  I  L  G  A  I  L  V

     2080      2090      2100      2110      2120      2130      2140      2150      2160
tggtagccggcctctggtggctgatcagccgtcgcaaaaagcgttccgcttaataagattcaaggtcaaaatcatgtctaatgaaacgc
  V  A  G  L  W  W  L  I  S  R  R  K  K  R  S  A  *                    M  S  N  E  T  L
                                                                                  FdhL (Subunit I)

     2170      2180      2190      2200      2210      2220      2230      2240      2250
tttcggctgatgtcgtcatcattggagcaggaatctgcggctccctgctcgcccacaaactcgtccgcaacggactttctgtgctgctcc
  S  A  D  V  V  I  I  G  A  G  I  C  G  S  L  L  A  H  K  L  V  R  N  G  L  S  V  L  L  L

     2260      2270      2280      2290      2300      2310      2320      2330      2340
tggatgcaggtccccgccgggaccgctcccagatcgtagaaaactggcggaacatgccgcctgacaacaagtcccagtacgattatgcaa
  D  A  G  P  R  R  D  R  S  Q  I  V  E  N  W  R  N  M  P  P  D  N  K  S  Q  Y  D  Y  A  T

     2350      2360      2370      2380      2390      2400      2410      2420      2430
caccttaccccagcgtaccctgggccccgcataccaactacttcccagacaataactacctgattgtcaaaggcccggaccggacggctt
  P  Y  P  S  V  P  W  A  P  H  T  N  Y  F  P  D  N  N  Y  L  I  V  K  G  P  D  R  T  A  Y
```

```
     2440      2450      2460      2470      2480      2490      2500      2510      2520
acaagcaaggaatcatcaaaggcgtcgggggtacaacctggcactgggcggcttcaagctggcggtacctgcccaacgatttcaagctgc
  K  Q  G  I  I  K  G  V  G  G  T  T  W  H  W  A  A  S  S  W  R  Y  L  P  N  D  F  K  L  H

     2530      2540      2550      2560      2570      2580      2590      2600      2610
attccacatatggcgtgggccgcgattacgccatgagctacgacgaacttgagccttactattacgaggccgagtgcgaaatgggcgtga
  S  T  Y  G  V  G  R  D  Y  A  M  S  Y  D  E  L  E  P  Y  Y  Y  E  A  E  C  E  M  G  V  M

     2620      2630      2640      2650      2660      2670      2680      2690      2700
tgggaccaaacggcgaagagattacaccgtctgcgcctcgccaaaatccatggccgatgacctccatgccttacggatatggagaccgca
  G  P  N  G  E  E  I  T  P  S  A  P  R  Q  N  P  W  P  M  T  S  M  P  Y  G  Y  G  D  R  T

     2710      2720      2730      2740      2750      2760      2770      2780      2790
ctttcacggagatcgtcagcaagctcggtttctcaaacactcctgttccgcaggcacggaacagtcgtccttatgatggccgaccacaat
  F  T  E  I  V  S  K  L  G  F  S  N  T  P  V  P  Q  A  R  N  S  R  P  Y  D  G  R  P  Q  C

     2800      2810      2820      2830      2840      2850      2860      2870      2880
gctgtggcaacaacaactgcatgccaatctgcccgattggcgcgatgtacaatggcgtatacgcggcaataaaagcggaaaagctgggcg
  C  G  N  N  N  C  M  P  I  C  P  I  G  A  M  Y  N  G  V  Y  A  A  I  K  A  E  K  L  G  A

     2890      2900      2910      2920      2930      2940      2950      2960      2970
caaaaattattcccaatgctgtcgtctatgcgatggaaacggatgcaaaaaaccggatcacagcgattagcttctatgatcccgacaagc
  K  I  I  P  N  A  V  V  Y  A  M  E  T  D  A  K  N  R  I  T  A  I  S  F  Y  D  P  D  K  Q

     2980      2990      3000      3010      3020      3030      3040      3050      3060
agtcccatcgcgtcgttgcaaaaacatttgtgatcgccgcaaacgggatcgaaacaccgaaactgctgcttctggcggcaaatgatcgaa
  S  H  R  V  V  A  K  T  F  V  I  A  A  N  G  I  E  T  P  K  L  L  L  L  A  A  N  D  R  N

     3070      3080      3090      3100      3110      3120      3130      3140      3150
accctcatgggattgccaactcatcagaccttgttggccggaacatgatggaccatccgggcatcggcatgagcttccagtctgcggagc
  P  H  G  I  A  N  S  S  D  L  V  G  R  N  M  M  D  H  P  G  I  G  M  S  F  Q  S  A  E  P

     3160      3170      3180      3190      3200      3210      3220      3230      3240
ccatctgggctggtggaggctcagtccagatgagttccatcaccaacttccgtgatggcgatttccgctcggagtatgctgccacgcaga
  I  W  A  G  G  G  S  V  Q  M  S  S  I  T  N  F  R  D  G  D  F  R  S  E  Y  A  A  T  Q  I

     3250      3260      3270      3280      3290      3300      3310      3320      3330
tcggctacaacaatacggcccagaactcacgcgccggcatgaaagctctgtccatggggttggttggcaagaagctggatgaagaaatcc
  G  Y  N  N  T  A  Q  N  S  R  A  G  M  K  A  L  S  M  G  L  V  G  K  K  L  D  E  E  I  R

     3340      3350      3360      3370      3380      3390      3400      3410      3420
gccgtcgtacggcgcatggtgtggacatttatgccaaccatgaagtcctcccggaccccaacaaccgtcttgttctctccaaagactata
  R  R  T  A  H  G  V  D  I  Y  A  N  H  E  V  L  P  D  P  N  N  R  L  V  L  S  K  D  Y  K

     3430      3440      3450      3460      3470      3480      3490      3500      3510
aggatgcgctcggtattccacatcctgaagtcacctacgatgttggggagtatgttcggaagtcagctgccatctcaagacagcgcctga
  D  A  L  G  I  P  H  P  E  V  T  Y  D  V  G  E  Y  V  R  K  S  A  A  I  S  R  Q  R  L  M

     3520      3530      3540      3550      3560      3570      3580      3590      3600
tggatatcgccaaagccatgggcggtacggaaatcgagatgactccgtattttacgcccaacaaccacatcaccggtggcactatcatgg
  D  I  A  K  A  M  G  G  T  E  I  E  M  T  P  Y  F  T  P  N  N  H  I  T  G  G  T  I  M  G
```

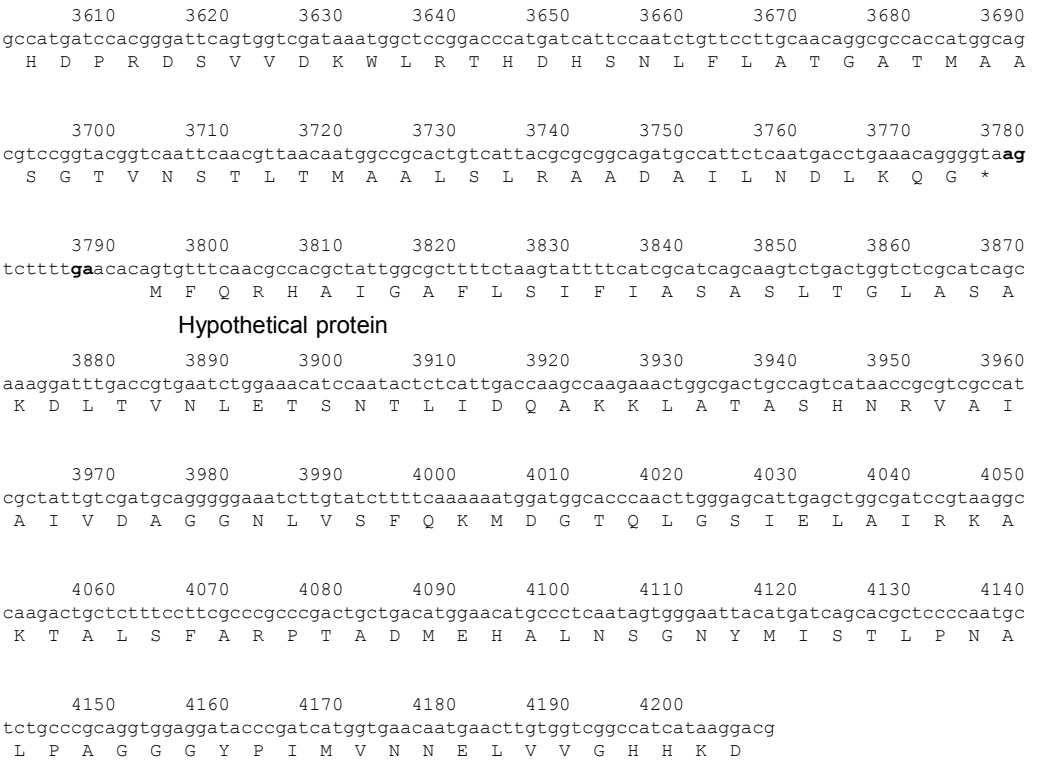

Figure S1. Nucleotide and predicted amino acid sequences of *fdhSCL* are shown. Part of the gene for a hypothetical protein downstream of *fdhL* is also shown. Possible ribosome-binding sites located prior to the initiation codon of each gene are shown in bold face. Consensus sequences for heme C binding and FAD binding are shown in bold face. Black arrowheads indicate putative cleavage sites for the precursor forms of subunits II and III, predicted by the SOSUIsignal program. The amino acid sequence of subunit I determined by the peptide sequencer is underlined. The nucleotide sequence and predicted amino acid sequences for *fdhSCL* were deposited to DDBJ with the accession number AB728565.

Chapter 2

The Electron Transfer Pathway in Direct Electrochemical Communication of Fructose Dehydrogenase with Electrodes

The author have constructed the expression system of subunit I/III subcomplex (FdhSL) lacking of the heme C subunit and partially purified it. FdhSL catalyzes the oxidation of D-fructose with several artificial electron acceptors, but loses the DET ability. The bi-molecular reaction rate constant (k) between FdhSL and *p*-benzoquinone (*p*BQ) derivatives was evaluated. The quinones work as non-specific electron acceptors of FdhSL. In contrast, FDH has some attractive interaction with 2,3-dimethoxy-5-methyl-*p*BQ derivatives. The formal potentials ($E^{\circ\prime}$) of the three heme C moieties in FDH have been determined to be –10 ± 4, 60 ± 8 and 150 ± 4 mV (vs. Ag|AgCl|sat. KCl) at pH 5.0, while the onset potential of FDH-catalyzed DET-type bioelectrocatalytic wave is –100 mV. Judging from these results, FDH communicates electrochemically with electrodes via the heme C with 60 ± 8 mV.

Introduction

Direct electron transfer (DET)-type bioelectrocatalysis is an intriguing phenomenon. DET reactions have the benefit to minimalize the loss of thermodynamic efficiency in bioelectrocatalytic reactions and may be utilized in several bioelectrochemical devices such as biofuel cells and biosensors [1,2]. Although DET bioelectrocatalysis is observed only for some limited redox enzymes, the interfacial electron transfer (ET) between electrodes and redox enzymes is one of the most important and interesting subjects in this field. There must be some factors of critical importance to govern DET reactions. However, the factors remain to be elucidated.

D-Fructose dehydrogenase (FDH; EC 1.1.99.11) from *Gluconobacter japonicus* NCBR 3260 is a heterotrimeric membrane-bound enzyme complex with a molecular mass of *ca*. 140 kDa, consisting of subunits I (67 kDa), II (51 kDa), and III (20 kDa). Subunits I and II have a covalently bound flavin adenine dinucleotide (FAD) and three heme C moieties, respectively. FDH shows strict substrate-specificity to D-fructose, and is utilized in diagnostic and food analyses [3,4]. On the other hand, FDH provides large catalytic current density in DET bioelectrocatalysis [5] as well as some hydrogenases [6,7]. It is thought that FDH reacts with electrodes at the heme C subunit [5], but no direct evidence has been reported to support the idea. In this chapter, the author has constructed subunit I/III subcomplex (FdhSL) that lacks subunit II containing the three heme C moieties, and compared the electrochemical features with those of FDH in order to examine the ET pathway from FDH to electrodes. Based on

bioelectrocatalytic kinetics, thermodynamics and protein engineering, the author will propose an idea that two of the three heme C moieties are involved in the catalytic cycle and the DET reaction, while the other heme with the highest formal potential remains reduced.

Experimental

Materials

$(NH_4)_2OsCl_6$, $Ru(NH_3)_6Cl_3$, 2,3-dimethoxy-5-methyl-1,4-benzoquinone (Q_0), and 2,3-dimethoxy-5-farnesyl-1,4-benzoquinone (Q_1) were obtained from Sigma-Aldrich Co. (USA). Na[Fe(edta)] (edta; ethylenediamine tetraacetate) was purchased from Dojindo Laboratory (Japan). Other chemicals were from Wako Pure Chemical Industries (Japan).

Purification of FDH and FdhSL

The expression and purification of FDH and FdhSL were carried out as described in a previous paper [8]. However, some modifications were done for the purification of the soluble FdhSL. In the literature [6], all of the solutions used for the purification contain TritonX-100 and mercaptoethanol, as in the case of the FDH purification. However, TritonX-100 may adsorb on electrodes and mercaptoethanol may form self-assembled layers on Au electrodes. Since these situations might inhibit DET reactions of redox proteins, the two reagents were removed from all of the solutions used for the purification of FdhSL. In brief, the freshly harvested cells were suspended with 20-fold-diluted McIlvaine buffer (pH 6.0) and then disrupted with a French pressure cell press (Thermo Fisher Scientific, Waltham, MA). The resulting lysate was centrifuged at 100,000×*g* for 1 h. The supernatant was applied to a DEAE-Sepharose column equilibrated with 20-fold-diluted McIlvaine buffer (pH 6.0). The purity of FdhSL was checked on SDS-PAGE by Coomassie brilliant blue R-250 staining.

Electrochemical measurements

Cyclic voltammetry was carried out in McIlvaine buffers (pH 5.0 and 6.0) at 25 °C on a BAS CV-50W electrochemical analyzer under anaerobic conditions. The working electrode was an Au electrode. The reference and counter electrodes were a handmade Ag|AgCl|sat.KCl electrode and a Pt wire, respectively. All the potentials are referred to the reference electrode in this chapter.

Spectroelectrochemical determination of protein redox potentials

The formal potentials of the hemes C in FDH were determined by a mediated spectroelectrochemical titration method according to the literature [9]. Mediated bulk

electrolysis was carried out at 25 °C on a BAS CV-50W electrochemical analyzer under stirring and anaerobic conditions in McIlvaine buffer (pH 5.0) containing 0.3% (w/w) Antifoam PE-L (Wako Pure Chem., Japan) as an antifoaming reagent. Spectral change of the electrolysis solutions was monitored on a MultiSpec-1500 photodiode array (Shimadzu, Japan). The redox mediators used were 200 μM $Ru(NH_3)_6Cl_3$ (E_m = –172 mV; E_m being the midpoint potential determined with cyclic voltammetry at pH 5.0), 200 μM Na[Fe(edta)], (E_m = –91 mV); 200 μM $(NH_4)_2OsCl_6$ (E_m = 35 mV), and 100 μM $K_3[Fe(CN)_6]$ (E_m = 225 mV).

Results and discussion

The electrochemical features of FDH and FdhSL

The author constructed a strain to produce FdhSL and partially purified FdhSL in the absence of TritonX-100 and mercaptoethanol. The concentration of the partially purified FdhSL was spectrophotometrically determined using an extinction coefficient of free FAD (11,300 M^{-1} cm^{-1} [10]). D-Fructose oxidation activity of FdhSL was measured with $K_3[Fe(CN)_6]$ as an electron acceptor as described in the literature [3]. FdhSL shows a high activity to oxidize D-fructose of 40 ± 3 U mg^{-1} at the optimum pH (6.0), which is compared with that of FDH (260 ± 20 U mg^{-1} at the optimum pH (5.0)).

However, in contrast to FDH, any DET catalytic current was not observed with FdhSL (even at *ca.* 3 μM) at a bare Au electrode (in the presence of 0.2 M D-fructose, Fig. 1A). FDH loses the DET activity by removing the heme C subunit. When *p*-benzoquinone (*p*BQ) was added in the electrolysis solution containing FdhSL and D-fructose, a clear catalytic current of D-fructose oxidation was observed (Fig. 1A), in which *p*BQ works as an ET mediator.

The bi-molecular reaction rate constant (k (=k_{cat}/K_M)) between FdhSL and the quinones was assessed from the dependence of the limiting catalytic current (I_s^{lim}) on the quinone concentration according to the literature [11]. k_{cat} and K_M are the catalytic constant and the Michaelis constant for the mediator, respectively. When $c_M/K_M << 1$, the I_s^{lim} is expressed by Eq. (1),

$$I_s^{lim} = n_M F A c_M \sqrt{\left(\frac{n_S}{n_M}\right) D_M k c_E} \quad (1)$$

where n_M and n_S are the electron number of mediator and substrate, respectively. F and A are the Faraday constant and electrode surface area. D_M, c_M and c_E are the diffusion coefficient of mediator, the bulk concentration of enzyme. The I_s^{lim} value increases linearly with c_E. Indeed, the I_s^{lim} of FdhSL increased linearly along with the concentration of *p*BQ on linear

sweep voltammogram (Fig. 2B) The log(k) values with the quinones were plotted against E_m of the quinones by analyzing the I_s^{lim} using Eq. (1) (Fig. 3). The log(k) values increase linearly with E_m of the quinone with a slope of 30 mV^{-1}. This property is called linear free energy relationships (LFER) observed for non-specific interactions of a series of related compounds with the identical main structure. Figure 4 shows a schematic diagram of reaction energy map to explain LFER. $\Delta G°$ and $\Delta G°^{‡}$ represent the Gibbs free energy and the activation free energy in Fig. 4, respectively. The subscripts 1 and j indicate a series of non-specific compounds involved in a similar reaction. Here, we may define $\Delta G°$ and $\Delta G°^{‡}$ as Eq. (2).

$$\Delta G°^{‡}_{j} - \Delta G°^{‡}_{1} \equiv \Delta\Delta G°^{‡}, \quad \Delta G°_{j} - \Delta G°_{1} = \Delta\Delta G° \tag{2}$$

As can be expected from the diagram, $\Delta\Delta G°$ has a linear relation with $\Delta\Delta G°^{‡}$.

$$\Delta\Delta G°^{‡} = \beta\Delta\Delta G° \quad (0 < \beta < 1) \tag{3}$$

where β is the coefficient and $\beta = 0.5$ when $\theta_1 = \theta_2$; $1 > \beta > 0.5$ when $\theta_1 > \theta_2$, and $0.5 > \beta > 0$ when $\theta_1 < \theta_2$. (4)

From the transition state theory, the reaction rate constant is related to $\Delta G°^{‡}$.

$$\ln k = -\Delta G^{°‡} / RT + \text{const.} \tag{5}$$

From the thermodynamic theory, the equilibrium constant is related to $\Delta G°$.

$$\ln K = -\Delta G^{°} / RT \tag{6}$$

Combining Eqs. (3)–(6), the author can get Eq. (7)

$$\ln\left(\frac{k_j}{k_1}\right) = \frac{-\Delta G°^{‡}_{j} - (-\Delta G°^{‡}_{1})}{RT} = -\frac{\Delta\Delta G°^{‡}}{RT} = -\beta\frac{\Delta\Delta G°}{RT} = \beta\frac{-\Delta G°_{j} - (-\Delta G°_{1})}{RT} = \beta\ln\left(\frac{K_j}{K_1}\right) \tag{7}$$

The $\Delta\Delta G°$ is related to $-nF\Delta E_M°$ in anodic mediated bioelectrocatalysis for a given enzyme, where n is the number of electron in the rate determining step and $\Delta E_M° = \Delta E_{M,j}° - \Delta E_{M,1}°$, $E_{M,j}°$ being the formal potential of mediator j. Therefore, the author can get:

$$\log\left(\frac{k_j}{k_1}\right) = \frac{\beta nF\Delta E_M°}{2.303RT} \tag{8}$$

Since the slope is given by $\beta nF/(2.303RT)$ in Fig. 3A, β is evaluated to be 0.5 by assuming n = 1. Thus the author can conclude that the pBQs work as non-specific electron acceptors of FdhSL.

The k values between FDH and the pBQs were also evaluated in a similar manner based on MET reaction, where TritonX-100 (1% as a final concentration) was added in the electrolyte solution to inhibit the DET reaction (Fig. 2C). It is very interesting that the log(k) values of Q_0 and Q_1 are obviously larger than those expected from the LFER characteristics observed for FdhSL (Fig. 3B, where the broken line represents a tentative one based on the characteristics of FdhSL). The heme C subunit is essential to bind FDH to the membrane and for *in vivo* fructose oxidizing respiratory activity [3]. Then the author can conclude that the electron-donating site of FDH locates on the heme C subunit. In addition, some ubiquinone in

the membrane is the most plausible natural electron acceptor of FDH. These considerations and the present results suggest that some specific attractive interaction occurs between the methoxy groups on the 2 and/or 3 positions of *p*BQ derivatives and the heme C moiety of FDH.

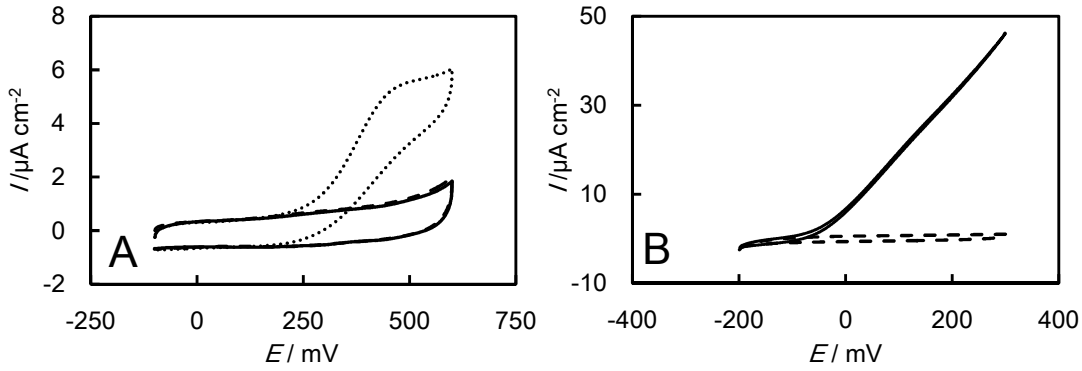

Figure 1. (A): Cyclic voltammograms (CVs) of fructose oxidation (0.2 M) catalyzed by (A) FdhSL (pH 6.0) and (B) FDH (pH 5.0) at $v = 10$ mV s^{-1} and at an Au electrode. Dash line: fructose only, solid line: enzyme + fructose, dotted line: enzyme + *p*BQ + fructose.

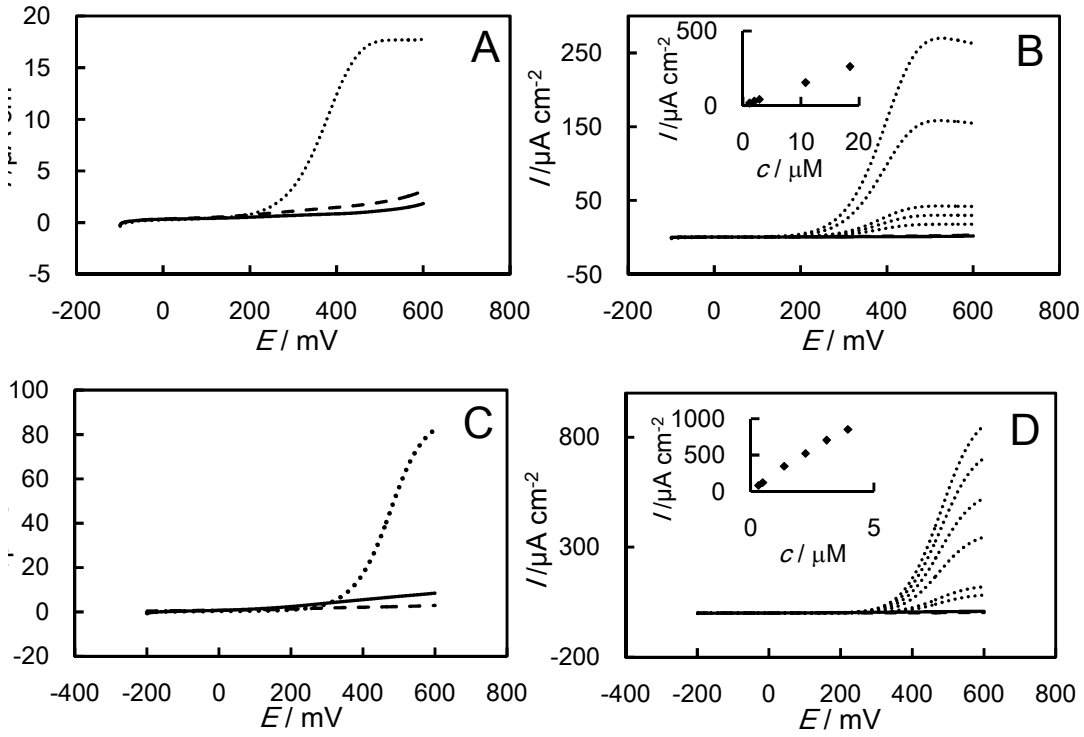

Figure 2. Linear sweep voltammograms of (A), (B) FdhSL and (C), (D) FDH at an Au electrode, scan rate = 10 mV s^{-1}. The SLVs were measured in McIlvaine buffer (A), (B) pH 6.0 (as the optimum pH of FdhSL) and (C), (D) pH 5.0 containing 1% TritonX-100 (as the optimum pH of FDH) containing 0.2 M fructose. Dashed line: background current in the absence of FDH or FdhSL, solid line: in the presence of FDH or FdhSL, dotted line: in the presence of benzoquinone as a mediator at several concentrations. Inset at panel (B) and (D): The plots of the observed current density at 600 mV against the final concentration of benzoquinone.

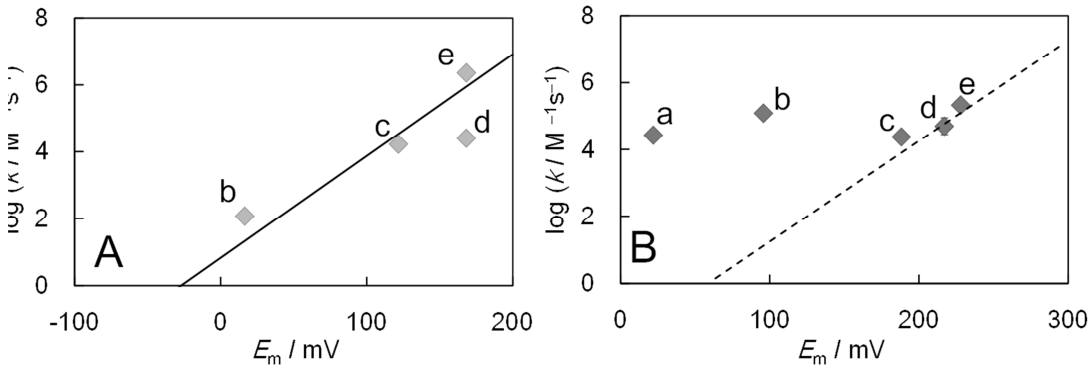

Figure 3. Bi-molecular rate constant (k) between the D-fructose-reduced enzymes ((A): FdhSL at pH 6.0 and (B): FDH at pH 5.0 in the presence of 1% TritonX-100) and *p*BQ derivatives as a function of the midpoint potential (E_m) of the quinones. The linear line in panel A indicates the linear-regression result: $\log(k) = (30 \pm 1) \times E_m$ [in mV] + 0.83 ± 1.3. The electron acceptors used are: (a) 2,3-dimethoxy-5-farnesyl-*p*BQ (Q_1), (b) 2,3-dimethoxy-5-methyl-*p*BQ (Q_0), (c) phenyl-*p*BQ, (d) *p*BQ, and (e) 2,5-dichloro-*p*BQ. The broken line in panel B is a tentative LFER line with a slope identical with that of the regression line in Fig. 2A. Q_1 reacts with FdhSL, but the rate constant is too small to be evaluated by voltammetry.

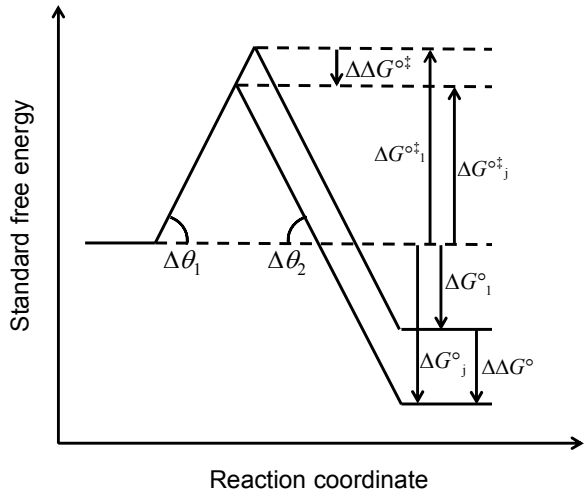

Figure 4. a schematic diagram of reaction energy map to explain linear free energy relationship

The formal potential of the three heme C moieties in FDH

The author determined the formal potential ($E°'$) of the three heme C moieties in FDH at pH 5.0 using a spectroelectrochemical method based on mediated bulk electrolysis [9]. Figure 5A shows the spectral change on bulk electrolysis of FDH at stepwise constant-potentials from –200 mV to 150 mV. Clear isosbestic points are observed in the wavelength region from 500 nm to 600 nm, where no absorption band appears for the mediators used. The spectral change is assigned to the redox reaction of the heme C moieties in FDH. In this work, the following sequential three-step one-ET model was used for the spectral analysis;

$Ox + e^- \rightleftarrows Red_1$ ($E_1°'$) (the first step at heme C_1) (9a)

$Red_1 + e^- \rightleftarrows Red_2$ ($E_2°'$) (the second step at heme C_2) (9b)

$Red_2 + e^- \rightleftarrows Red_3$ ($E_3°'$) (the third step at heme C_3) (9c)

where Ox, Red_1, Red_2 and Red_3 denote the fully oxidized, heme C_1-reduced, heme C_1, C_2-reduced and the fully reduced forms, respectively, and $E_1°'$, $E_2°'$, and $E_3°'$ are $E°'$s of the microscopic formal potentials of the first, second, and third step ETs, respectively. The Nernst equation of each step is given by:

$$\frac{[Ox]}{[Red_1]} = \exp[\frac{F}{RT}(E_s - E_1°')] \equiv \eta_1 \quad (10)$$

$$\frac{[Red_1]}{[Red_2]} = \exp[\frac{F}{RT}(E_s - E_2°')] \equiv \eta_2 \quad (11)$$

$$\frac{[Red_2]}{[Red_3]} = \exp[\frac{F}{RT}(E_s - E_3°')] \equiv \eta_3 \quad (12)$$

where E_s is the solution potential. By assuming identical spectroscopic characteristics of the three heme C moieties, the absorbance (A) is given by:

$$A = \{3\varepsilon_{ox}[\mathrm{Ox}] + (2\varepsilon_{ox} + \varepsilon_{red})[\mathrm{Red}_1] + (\varepsilon_{ox} + 2\varepsilon_{red})[\mathrm{Red}_2] + 3\varepsilon_{red}[\mathrm{Red}_3]\}\ell \quad (13)$$

where ε_{ox} and ε_{red} are the absorption coefficients of the oxidized and reduced forms of one heme C moiety at 550 nm, respectively, and ℓ is the light-path length. Combining Eqs. (10)–(13), the author can get Eq. (14) with c as the total concentration of the enzyme.

$$A = \{\frac{\varepsilon_{ox}(3\eta_1\eta_2\eta_3 + 2\eta_2\eta_3 + \eta_3) + \varepsilon_{red}(\eta_2\eta_3 + 2\eta_3 + 3)}{\eta_1\eta_2\eta_3 + \eta_2\eta_3 + \eta_3 + 1}\}c\ell \quad (14)$$

Thus the reduction ratio (R) defined as $R = \{[\mathrm{Red}_1] + 2[\mathrm{Red}_2] + 3[\mathrm{Red}_3]\}/3c$ is experimentally assessed by

$$R = \frac{A - A_O}{A_R - A_O} \quad (15)$$

where A_O and A_R are A at $E_s >> E_1°'$ and A at $E_s << E_3°'$, respectively.

The E_s-dependence of A at 550 nm was analyzed using Eqs. (14) and (15) based on a non-linear least square method using a free soft GNUPLOT [8]. The values were evaluated to be $E_1°' = 150 \pm 4$ mV, $E_2°' = 60 \pm 8$ mV, and $E_3°' = -10 \pm 4$ mV. These values may be compared with the onset potential of the DET reaction of FDH (*ca.* –100 mV at pH 5.0 [5, 12] (Fig. 1B). Since the $E°'$ of the electron-donating site should be located close to the onset potential of the DET-type bioelectrocatalytic wave, heme C_1 with $E_1°'$ seems to be ruled out as a candidate of the electron-donating site, because the uphill ET from 150 to –100 mV seems to be very difficult. Most probably, the two electrons from fructose are transferred to heme C_2 with $E_2°'$ and heme C_3 with $E_3°'$, and the heme C_2 seems to be the electron-donating site in the DET reactions. During the catalytic cycle, heme C_1 with $E_1°'$ remains reduced in our model. Actually, all of the three heme C moieties are fully reduced on the addition of D-fructose in the absence of electron acceptor, as judged from the spectroscopic data (data not shown).

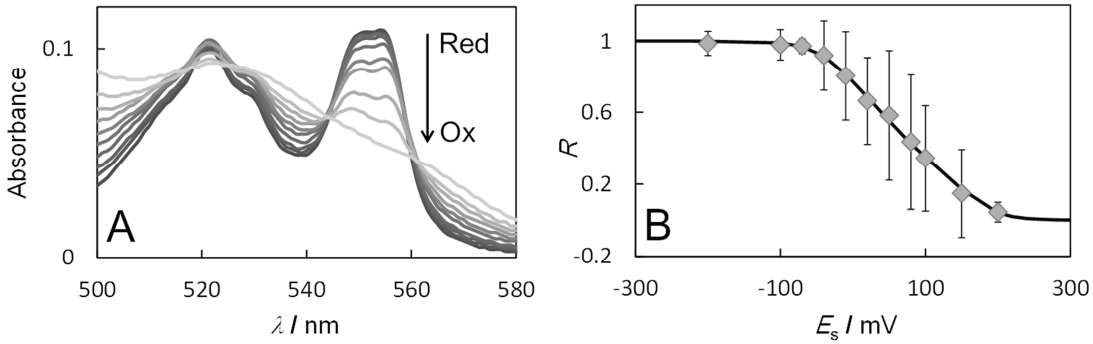

Figure 5. (A): Absorption spectral change of FDH solution in mediated spectroelectrochemical titration method without background subtraction. The mediators used for the bulk electrolysis were: 200 μM $Ru(NH_3)_6Cl_3$, 200 μM $(NH_4)_2OsCl_6$, 200 μM Na[Fe(edta)], and 100 μM $K_3[Fe(CN)_6]$. The electrolysis solution were equilibrated electrochemically at −200, −100, −70, −40, −10, 20, 50, 80, 100, and 150 mV from (Red to Ox in tern). Measurements were carried out in McIlvaine buffer (pH 5.0) under anaerobic conditions at 25 ˚C. (B): Nernst analysis of the solution potential (E_s)-dependence of the absorbance at 550 nm in Panel A. The error bars were evaluated by the Student *t*-distribution with a 90%-confidence level from 7 times of independent experiments. The solid regression curve was evaluated by a non-linear least-square method based on Eqs. (14) and (15).

References

[1] J. A. Cracknell, K. A. Vincent, F. A. Armstrong, Chem. Rev. 108 (2008) 2439.

[2] L. Gorton, A. Lindgren, T. Larsson, F.D. Munteanu, T. Ruzgas, I. Gazaryan, Anal. Chim. Acta. 400 (1999) 91.

[3] M. Ameyama, E. Shinagawa, K. Matsushita, O. Adachi, J. Bacteriol. 145 (1981) 814.

[4] K. Nakashima, H. Takei, O. Adachi, E. Shinagawa, M. Ameyama, Clin. Chim. Acta. 151 (1985) 307.

[5] Y. Kamitaka, S. Tsujimura, and K. Kano, Chem. Lett. 36 (2007) 218.

[6] A. K. Jones, E. Sillery, S. P. J. Albracht, and F. A. Armstrong, Chem. Commun. 8 (2002) 866.

[7] A. Parkin, G. Goldet, C. Cavazza, J. C. Fontecilla-Camps, and F. A. Armstrong, J. Am. Chem. Soc. 130 (2008) 40.

[8] S. Kawai, M. Tsutsumi, T. Yakushi, K. Kano, and K. Matsushita, Appl. Environ. Microbiol. 79 (2013) 1654.

[9] S. Tsujimura, A. Kuriyama, N. Fujieda, K. Kano, and T. Ikeda, Anal. Biochem. 337 (2005) 325.

[10] W. C. Kenney, D. E. Edmondson, and R. L. Seng, J. Biol. Chem. 251 (1976) 5386.

[11] R. Matsumoto, K. Kano, and T. Ikeda, J. Electroanal. Chem. 535 (2001) 37.

[12] M. Tominaga, C. Shirakihara, and I. Taniguchi, J. Electroanal. Chem. 610 (2007) 1.

Chapter 3

Electrochemical Characterization on the Reconstruction of the Subunits of Heterotrimeric Fructose Dehydrogenase

D-Fructose dehydrogenase (FDH) is heterotorimeric membrane-bound enzyme and one of the DET-type enzymes. It is high possibility that the subunit II, which has three heme C moieties, has key role for DET reaction, because subunit I/III subcomplex (FdhSL) lacking of the heme C subunit lose the DET ability. In this chapter, the author has constructed the expression system of the heme C subunit (FdhC). The non-turnover signal from FdhC on voltammogram was not observed. Judging from gel filtration column chromatography result, FdhC forms more than tetramer. The aggregation of FdhC might disturb the DET reaction of FdhC. In contrast, when FdhSL and FdhC were mixed, they were bound stoichiometrically 1 to 1 and the mixing solution showed fructose-oxidation catalytic current. The results strongly support that the heme C in FdhC is the reaction center in DET reaction of FDH.

Introduction

D-Fructose dehydrogenase (FDH; EC 1.1.99.11) was isolated from *Gluconobacter japonicas* (Former name: *Gluconobacter frateurii*) NBRC3260 as a heterotorimeric membrane-bound enzyme [1]. FDH catalyzes the oxidation of D-fructose to produce 5-keto-D-fructose. Subunit I (67 kDa) and II (51 kDa) has FAD and three heme C moieties as redox prosthetic groups, respectively [1,2]. Subunit III (20 kDa) has no cofactor and is presumed to be relating to the stability of FDH. FDH works as the primary dehydrogenase in the respiratory chain, where FDH oxidizes fructose and transfers the electrons to ubiquinone embedded in the membrane. FDH has strict substrate specificity on fructose as the electron donor, while FDH transfers the electron to several artificial electron acceptors [2]. FDH-catalyzed reaction is coupled with electrode reaction, because the oxidized artificial electron acceptors can be reduced by electrode. This reaction is called mediated electron transfer (MET)-type bioelectrocatalysis reaction. There are some reports about the determination of fructose in food and diagnostic analysis based on MET reaction of FDH [3, 4].

There is another method for coupling enzymatic reaction with electrode reaction in which redox enzymes react with electrode directly. This reaction is called direct electron transfer (DET)-type bioelectrocatalysis reaction. There is limited number of redox enzymes occurring DET reaction [5-9]. FDH is one of the DET-type enzymes [10]. The DET activity of FDH is quite high in comparison with that of alcohol dehydrogenase, which has many similar

characters to FDH [12,13]. The biofuel cell based on DET reaction of FDH as an anode has achieved the power density of 2.6 mW cm^{-2} [13]. There must be some factors of critical importance to govern DET reactions. The factors remain to be elucidated. Previously, the author reported that heme C in FDH works as reaction center with electrode, because subunit I/III subcomplex (FdhSL) lacking of the heme C subunit losts DET activity [14]. It is high possibility that the heme C subunit (FdhC) has the key role in DET reaction of FDH. However, the non-turnover signal, which might be observed when DET-type enzyme is absorbed on an electrode and there is no substrate, is not observed on voltammogram.

The signal is usually a pair of peaks from oxidation and reduction of the redox center. There are many researches that the redox peaks of horse heart cytochrome *c* (Cyt *c*) are observed on voltammograms [15-17]. Cyt *c* is a small heme protein with the molecular mass of *ca*. 12 kDa and shuttles electron in the process of respiratory chain [18,19]. The three-dimensional structure of cyt *c* has been published [18]. Cyt *c* has a spherical shape (2.6 × 3.2 × 3.0 nm) [20]. The size of DET-type proteins is one of the important factors for DET reaction, because DET reaction usually requires the adsorption of proteins on the electrode surface. However, DET-type proteins are not always small enough to observe the redox peak from them on voltammogram.

In this chapter, the author has constructed the expression system of subunit II (FdhC) of FDH. The crystal structure of FDH has not been elucidated. Shirakihara *et al*. reported the size of FDH with atomic force microscopic images is *ca*. 7 nm [21]. There is probably little possibility to observe the redox peaks from FDH on voltammogram, because the size of FDH is too big to observe the peaks. FdhC may be smaller than original FDH complex. The author attempts to demonstrate the redox behavior of FdhC and repair catalytic DET activity of FdhSL by binding FdhC.

Experimental

Bacterial strains, plasmids and growth conditions

Gluconobacter spp. were grown on ΔP medium, consisting of 5 g of glucose, 20 g glycerol, 10 g of hipolypeptone and 10 g of yeast extract per litter at 30 °C. The pSHO8 [2], a fragment of a putative promoter region of the *adhAB* gene of *G. oxydans* 621H was inserted into the broad-host-range vector pBBR1MCS-4, was used as the expression vector. *Escherichia coli* DH5α was used for plasmid construction [22]. *E. coli* HB101 harboring pRK2013 [23] was used as a helper strain for conjugative plasmid transfer. *E. coli* was grown in Luria broth at 37 °C.

Chemicals

Restriction endonucleases were purchased from TaKaRa Shuzo (Japan). Yeast extract was purchased from Oriental Yeast (Japan). 2,3-Dimethoxy-5-farnesyl-1,4-benzoquinone (Q_1) was obtained from Sigma-Aldrich Co. (USA). 2-Mercaptoetahnol was purchased from Nacalai tesque (Japan). Other chemicals were from Wako Pure Chemical Industries (Japan).

Exprssion of Subunit I/III complex (FdhSL) and subunit II (FdhC)

The expression of FdhSL was carried out as described in a previous paper [2]. The *fdhC* gene was amplified with Herculase II Fusion DNA Polymerase (STRATAGENE) using two phosphorylated primers (5'-gaattcATGCCGGCATTTTAAG-3' and 5'-ggatCCTTGAATCTTATTAAGC-3'; the residues printed in capital letters being complementary to the template sequence) from the genome DNA of *G. japonicus* NBRC3260 by polymerase chain reaction (PCR). The PCR product was inserted into pSHO8 [2] treated with *Eco*RI and *Bam*HI to yield pSHO21. The nucleotide sequence was confirmed by Fasmac sequencing service (Kanagawa, Japan). *G. oxydans* NBRC12528 ΔadhA::Km^r was transformed with pSHO21 as described in a previous paper [2].

Purification of FdhSL and FdhC

Gluconobacter harboring pSHO16 and pSHO21 were used for purification of FdhSL and FdhC, respectively. *Gluconobacter* cells were collected, suspended and then disrupted with a French pressure cell (Otake Works, Japan) as described by Kawai *et al.* [2]. The ultracentrifugation at 100,000 × *g* divided the resulting lysate into the supernatant fraction and the membrane fraction. The supernatant and membrane fraction were used for FdhSL and FdhC, respectively, because FdhC is membrane-anchoring region and FdhSL is soluble enzyme [2].

FdhSL is soluble enzyme [2]. The supernatant was applied to a DEAE-Shepharose Fast Flow column equilibrated with 20-fold-diluted MacIlvaine buffer (pH6.0). FdhSL was eluted with a linear gradient of from 20-fold-diluted to the original concentrations of MacIlvaine buffer (pH 6.0). The fractions containing FdhSL was collected. Ammonium sulfate (50% saturation) was added into the fractions. The supernatant was collected by centrifugation at 10,000 × *g* at 4 °C for 30 min after stirring at 4 °C for 1 h and applied to a Buthyl Toyopearl 650 M column equilibrated with 50 mM sodium phosphate buffer (NaPB) (pH6.0). The elution of FdhSL was carried out with a linear gradient from 50% to 0% saturated ammonium sulfate. The sample was concentrated and dialyzed overnight against 50 mM NaPB (pH 6.0) containing 150 mM NaCl. After dialysis, the sample was further purified by size exclusion chromatography on a Superdex-200 column equilibrated with 50 mM NaPB containing 150 mM NaCl.

FdhC is the membrane-anchoring region [2]. The membrane fraction after

ultracentrifugation of the lysate was suspended in 20-fold-diluted MacIlvaine buffer (pH 6.0) containing 1% TritonX-100, 1 mM 2-mercaptoethanol and 1 M KCl and stirred at 4 °C for 1 h. The solubilized supernatant was collected by ultracentrifugation at 100,000 × *g*. The supernatant was precipitated with 30% ammonium sulfate. The precipitate was dissolved in 20-fold-diluted MacIlvaine buffer (pH 5.0) containing 0.1% TritomX-100 and 1 mM 2-mercaptoethanol and dialyzed overnight against the same buffer. All of the solutions used for the purification of FdhC contain 0.1% TritonX-100 and 1 mM 2-mercaptoethanol. After dialysis, the sample was applied to a CM-Toyopearl column equilibrated with 20-fold-diluted MacIlvaine buffer (pH 5.0). FdhC was eluted with a linear gradient from 20-fold-diluted to the original concentrations of MacIlvaine buffer (pH 5.0). The fractions was collected, concentrated and dialyzed against 50 mM NaPB (pH 6.0).

The purity of FdhSL and FdhC were checked on SDS-PAGE by Coomassie brilliant blue R-250 staining. The concentrations of FdhSL and FdhC were spectrophotometrically determined using an extinction coefficient of free FAD (11,300 $M^{-1}cm^{-1}$ [24]) and heme C in FDH (23,000 $M^{-1}cm^{-1}$ [25]).

Electrochemical measurements

Cyclic voltammetry and linear sweep voltammetry were carried out in McIlvaine buffers (pH 5.0 or 6.0) at 25 °C on a BAS CV-50W electrochemical analyzer under anaerobic conditions. The working electrode was a Glassy carbon (GC) or Au electrode. The reference and counter electrodes were a handmade Ag|AgCl|sat.KCl electrode and a Pt-wire, respectively. All the potentials are referred to the reference electrode in this paper.

Results and discussion

Construction and expression of FdhSL and FdhC

The author has previously reported the expression and partially purification of FdhSL [2]. The author carried out the purification of FdhSL by the previously reported method [14] with some modifications and succeeded in more high purification of FdhSL in this paper. The specific activity was improved from 40 ± 3 U mg^{-1} to 75 ± 10 U mg^{-1} at the optimum pH 6.0 [14]. The purified FdhSL had a clear FAD signal by UV-vis spertroscopy measurement and two major bands on SDS-PAGE by Coomassie brilliant blue R-250 staining (data not shown). The concentration of FdhSL was calculated from the extinction coefficient of free FAD. The value was 8.2 μM.

The *FdhC* gene was inserted into pSHO8 and the author yielded pSHO21. The cells harvesting pSHO8 and pSHO21 were cultured, collected and disrupted. The SDS-PAGE

electrophoresis was performed by using the membrane fractions of the strains harvesting pSHO8 and pSHO21for confirming the expression of FdhC. Heme-catalyzed peroxidase staining of the SDS-PAGE gel showed only approximately 50 kDa band with the pSHO21-membrane fraction, while there was no stained band on SDS-PAGE gel with the pSHO8-membrane fraction. This result suggests that most of protein having heme C in pSHO21-membrane fraction is from FdhC. The author purified FdhC and calculated from the extinction coefficient of heme C in FDH that the concentration of FdhC was 35 μM.

The electron transfer between FdhSL and FdhC

The redox state of heme C moieties in FdhC was monitored in the McIlvaine buffer (pH 5.0) on a MultiSpec-1500 photodiode array (Shimadzu, Japan). Potassium ferricyanide was added in the measurement solution in order to fully oxide heme C moieties in FdhC (Fig. 1 black solid line). After addition of either FdhSL or frucotose, FdhC maintained oxidized form. In contrast, the addition of both FdhSL and fructose reduced FdhC moieties (Fig. 1 gray solid line). There was no absorption spectra change by further addition of sodium dithionite as a reducing agent. The spectra change means that all three heme C moieties in FdhC are reduced by FdhSL-catalyzed fructose oxidation reaction.

Cyclic voltammetry was performed in the McIlvaine buffer (pH 5.0) by using GC electrode as a working electrode. There were no clear redox peaks from FdhC after addition of FdhC solution (Fig. 2A). The author also measured the CV by using self-assembled monolayer (SAM) modified Au electrodes as working electrode in same manner of using GC electrode. Four types of thiols for constructing SAM-modified electrodes and controlling the orientation of FdhC on the electrodes were used. SAM-modified Au electrodes were prepared by immersing Au electrode for at least 1 h in an ethanol solution or ultrapure water containing 1 mM of the corresponding thiol. Before measurements, SAM-modified Au electrodes were washed thoroughly with ethanol and ultrapure water in turn. The hydrophobicity of electrode surface was changed by using 2-mercapthoethanol and mercapthoethane. The charge of electrode surface was changed by using 2-aminoethonethiol hydrochloride and 3-mercapto-1-propanesulfonic acid. However, there were no signals from FdhC on the CVs with all SAM modified electrodes (data not shown).

FdhSL and FdhC previously were mixed. The CV was carried out with GC electrode in the McIlvaine buffer (pH 5.0) containing 200 mM fructose. After the mixed solution was added in the electrolyte solution, the fructose-oxidation catalytic current was observed (Fig. 2B). FdhSL has no DET activity [14]. The author has confirmed the ET reaction between FdhSL and FdhC occurred as above described. The results suggest that FdhC reacts with electrode, although no redox signal of FdhC on the CV was observed.

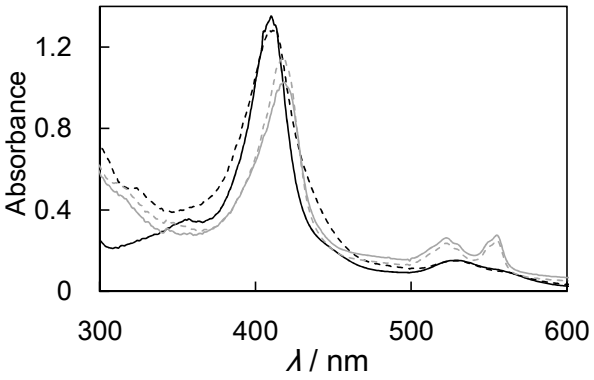

Figure 1. Absorption spectral change of FdhC solution in MacIlvaine buffer (pH 5.0). FdhC was fully oxidized by addition of potassium ferricyanide (solid black line). After then, FdhSL (dash black line), fructose (solid gray line) and sodium dithionite (dash gray line) were added in order.

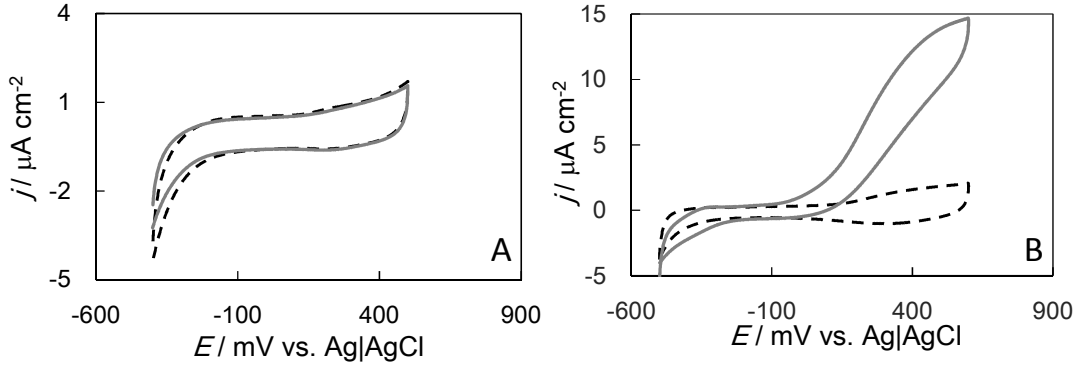

Figure 2. Cyclic voltammograms of FdhC (A) and the mixing solution of FdhSL and FdhC (B) in MacIlvaine buffer (pH 5.0) at v = 10 mV s^{-1} and at GC electrode. Dash line: background current in the absence of enzyme, solid line: in the presence of FdhC (A), in the presence of FdhSL, FdhC and fructose (B).

The aggregation of FdhC

The size of FdhC was measured by size exclusion chromatography on a Superdex-200 column. The column was equilibrated with 50 mM NaPB containing 150 mM NaCl and 0.1% TritonX-100. MW-marker (Oriental Yeast, Japan) was used as marker protein and 0.1% TritonX-100 was previously added in MW-marker solution. FdhC had about 230 kDa of

molecular mass measured by gel filtration column chromatography, while judging from amino acid sequence of FdhC, the molecular mass of FdhC is approximately 50 kDa. The author also measured molecular mass of FDH by gel filtration column chromatography. The molecular mass of FDH was about 290 kDa, which would be nearly corresponding to dimer of FDH. It seems that FdhC forms tetramer or more multimer and is more aggregating than FDH. The aggregation of FdhC might disturb the proper orientated adsorption on the electrode for DET reaction. On the other hand, the aggregation of FdhC might be relaxed by the mixing of FdhSL and FdhC.

Titration of FdhSL and FdhC

The linear sweep voltammetry was performed from 0 mV to 600 mV at a scan rate of 10 mV s^{-1} in McIlvaine buffer (pH 5.0) containing fructose. Fig. 3A solid black line showed the voltammogram with addition of FdhSL and Q_1 in the measurement solution. We previously reported the bi-molecular reaction rate constant (k ($=k_{cat}/K_M$)) between FdhSL and *p*-benzoquinone derivatives from the limiting catalytic current on the voltammograms [14]. k_{cat} and K_M are the catalytic constant and the Michaelis constant for the mediator, respectively. FdhSL has non-specific interactions with *p*-benzoquinone derivatives with obeying linear free energy relationships (LFER). The log(k) values increase linearly with midpoint potential of the quinones with a slope of 30 mV^{-1}. The limiting current on Fig. 3A solid black line consists of a part of catalytic current and the rest of non-catalytic Q_1-oxidation current, because the log(k) value of Q_1 evaluated from LFER (less than 2.0) is too small for FdhSL quickly to reduce Q_1 in bulk during voltammetry. After FdhC was added in the measurement solution, a clear fructose-oxidation current was observed (Fig. 3A solid gray lines). The fructose-oxidation current was increased along with the increase of addition of FdhC and finally reached the ceiling fructose-oxidation current. The log(k) value of $Q_1$with FDH (more than 4.0) is much larger than that of evaluated from LFER [2]. It is high possibility that FdhC has the same interaction with Q_1 as like FDH and facilitates the ET reaction between FdhSL and Q_1. The final concentration of FdhC at reaching the ceiling catalytic current is too low to regard FdhC as an ET mediator.

When FdhSL and FdhC are bound by mixing them and $c_M/K_M << 1$, the limiting catalytic current (I_s^{lim}) is expressed by Eq. (1),

$$I_s^{lim} = n_M FAc_M \sqrt{\left(\frac{n_S}{n_M}\right) D_M kc_{FDH}} \quad (1)$$

where n_M and n_S are the electron number of mediator and substrate, respectively [26]. F

and A are the Faraday constant and electrode surface area. D_{M} , c_{FDH} and c_{M} are the diffusion coefficient of mediator, the bulk concentration of FDH constructed by mixing FdhSL and FdhC, and mediator. The Eq. (1) is transformed into:

$$c_{\mathrm{FDH}} = \frac{1}{n_{\mathrm{S}} n_{\mathrm{M}} k D_{\mathrm{M}}} \left(\frac{I_{\mathrm{s}}^{\lim}}{F c_{\mathrm{M}}} \right)^2 \tag{2}$$

The c_{FDH}-dependence of the additional molar amount of FdhC ($n_{\mathrm{C},0}$) to the initial molar amount of FdhSL ration ($n_{\mathrm{SL},0}$) in the measurement solution was plotted by analyzing the $I_{\mathrm{s}}^{\lim}$ of Fig. 3A using Eq. (2) (Fig. 3B). The c_{FDH} was increased approximately linearly with the increase the FdhC until stoichiometric ration of $n_{\mathrm{C},0} / n_{\mathrm{SL},0}$ reached about 1 to 1. After that, c_{FDH} was not increased in spite of the further addition of FdhC. The result suggests that FdhSL and FdhC are bound stoichiometrically 1 to 1. The log(k) value of $Q_1$with FDH was 3.8 ± 0.1. This value was smaller than that of original FDH complex. The stability of original FDH complex is quite high. When original FDH complex was stored in MacIlvaine buffer (pH 6.0) at 4 °C, the fructose-oxidation activity maintained more than 90% for few days. On the other hand, the stability of FdhSL was not as good as original FDH complex. When FdhSL was stored in the same conditions with FDH, the activity decreased to less than 90% for a day. It seems that FdhSL is slowly losing the activity during its purification. The author considers the difference of the log(k) value of Q_1 between original FDH complex and FDH which is constructed by mixing FdhSL and FdhC causes by the stability of FdhSL.

Let him consider the binding constant (K_{b}) between FdhSL and FdhC.

$$K_b = \frac{c_{\mathrm{FDH}}}{c_{\mathrm{SL}} c_{\mathrm{C}}} \tag{3}$$

Where c_{SL} and c_{C} are the bulk concentration of FdhSL and FdhC. The initial molar amount of FdhSL ($n_{\mathrm{SL},0}$) is given by:

$$n_{\mathrm{SL},0} (= c_{\mathrm{SL},0} V_0) = n_{\mathrm{SLC}} + n_{\mathrm{SL}} \tag{4}$$

where n_{SLC} , n_{SL} are the bulk molar amount of FDH, which is constructed by joining FdhSL and FdhC, and FdhSL, which exist without binding with FdhC. $c_{\mathrm{SL},0}$ and V_0 are the initial

concentration of FdhSL and the initial measurement solution volume. On the other hand, the total added molar amount of FdhC ($n_{C,0}$) is given by:

$$n_{C,0}(=c_{C,0}\Delta V)=n_{FDH}+n_{C} \tag{5}$$

where n_{C} and ΔV are the bulk molar amount of FdhC, which exists without binding with FdhSL, and the additional volume of FdhC in measurement solution. Combining Eqs. (3)-(5), the author can get Eq. (6).

$$c_{SLC}=\frac{n_{FDH}}{V_0+\Delta V}=\frac{\alpha-\sqrt{\alpha^2-4K_b^2 n_{SL,0}n_{C,0}}}{2K_b(V_0+\Delta V)} \tag{6}$$

$$\alpha=K_b(n_{SL,0}+n_{C,0})+V_0+\Delta V \tag{7}$$

The c_{FDH}-dependence of $n_{C,0}/n_{SL,0}$ was analyzed using Eq. (6) based on non-linear least square method using a Microsoft Excel spreadsheet. K_b was evaluated to be 1×10^{14} M^{-1}. It is likely that FdhSL is strongly bound with FdhC and both of them hardly separate.

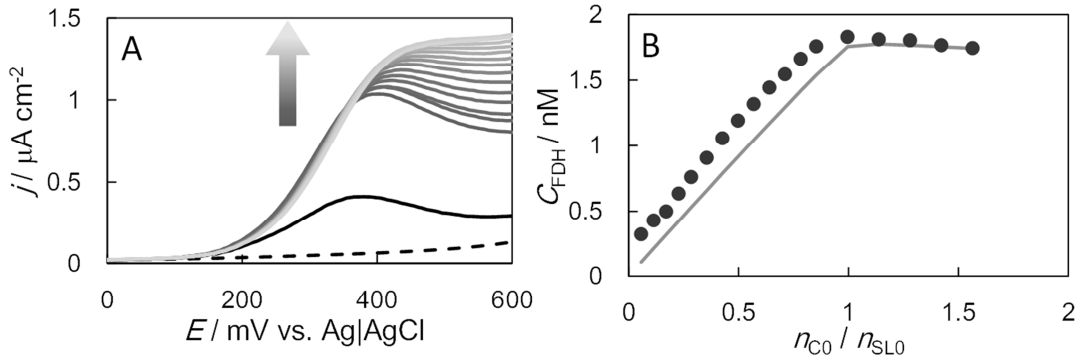

Figure 3. (A) Linear sweep voltammograms at an Au electrode, scan rate = 10 mV s^{-1}. The SLVs were measured in McIlvaine buffer (pH 5.0) containing 1% TritonX-100 and 200 mM fructose. Dash black dash line: background current, Solid black line: in the presence of FdhSL and Q1 as a mediator, dash gray lines: in the presence of FdhC at everal concentrations. (B) FDH concentration which was constructed by mixing FdhSL and FdhC as a function of the additional molar amount of FdhC to the initial molar amount of FdhSL ration in panel A. The solid gray line was evaluated by a non-linear least-square method based on Eqs. (6) and (7).

References

[1] M. Ameyama, E. Shinagawa, K. Matsushita, O. Adachi, J. Bacteriol. 145 (1981) 814.

[2] S. Kawai, M. Tsutsumi, T. Yakushi, K. Matsushita, K. Kano, Appl. Environ. Microbiol. 79 (2013) 1654.

[3] R. Antiochia, L. Gorton, Sens. Actuators B. 195 (2014) 287.

[4] T. Ikeda, F. Matsushita, M. Senda, Agric. Biol. Chem. 54 (1990) 2919.

[5] L. Gorton, A. Lindgren, T. Larsson, F. D. Munteanu, T. Ruzgas, I. Gazaryan, Analytica. Chimica. Acta. 400 (1999) 91.

[6] S. Tsujimura, T. Nakagawa, K. Kano, T. Ikeda, Electrochemistry 72 (2004) 437.

[7] A. Ciaccafava, P. Infossi, M. Ilbert, M. Guiral, S. Lecomte, M.T. Giudici-Orticoni, E. Lojou, Angew. Chem., Int. Ed. 50 (2011) 1.

[8] A. L. Ghindilis, P. Atanasov, E. Wilkins, Electroanalysis 9 (1997) 661.

[9] J. A. Cracknell, K. A. Vincent, F. A. Armstrong, Chem. Rev. 108 (2008)

2439.
[10] Y. Kamitaka, S. Tsujimura, K. Kano, Chem. Lett. 36 (2007) 218.
[11] T. Ikeda, D. Kobayashi, F. Matsushita, T. Sagara, K. Niki, J. Electroanal. Chem. 361 (1993) 221.
[12] O. Adachi, K. Tayama, E. Shinagawa, K. Matsushita, M. Ameyama, Agric. Biol. Chem. 42 (1978) 2045.
[13] K. So, S. Kawai, Y. Hamano, Y. Kitazumi, O. Shirai, M. Hibi, J. Ogawa, K. Kano, Phys. Chem. Chem. Phys. 16 (2014) 4823.
[14] S. Kawai, T. Yakushi, K. Matsushita, Y. Kitazumi, O. Shirai, K. Kano, Electrochem. Commun. 38 (2014) 28.
[15] F. A. Armstrong, H. Allen, O. Hill, N. J. Walton, Acc. Chem. Res. 21 (1988) 407.
[16] F. Schröper, A. Baumann, A. Offenhäusser, D. Mayer, Biosens. Bioelecron. 34 (2012) 171.
[17] L. Gorton, A. Lindgren, T. Larsson, F. D. Munteanu, T. Ruzgas, I. Gazaryan, Analytica. Chimica Acta. 400 (1999) 91.
[18] G. W. Bushnell, G. V. Louie, G. D. Brayer, J. Mol. Biol. 214 (1990) 585.
[19] F. S. Mathews, Prog. Biophys. Mol. Biol.45 (1985) 1.
[20] A. Vinu, V. Murugesan, O. Tangermann, M. Hartmann, Chem. Mater. 16 (2004) 3056.
[21] M. Tominaga, C. Shirakihara, I. Taniguchi, J. Electroanal. Chem. 610 (2007) 1.
[22] S. G. Grant, J. Jessee, F. R. Bloom, and D. Hanahan, Proc. Natl. Acad. Sci. U S A. 87 (1990) 4645.
[23] D. H. Figurski, D. R. Helinski, Proc. Natl. Acad. Sci. U S A. 76 (1979) 1648.
[24] W. C. Kenney, D. E. Edmondson, and R. L. Seng, J. Biol. Chem. 251 (1976) 5386.
[25] J. Marcinkeviciene and G. Johansson, 318 FEBS Lett. (1993) 23.
[26] R. Matsumoto, K. Kano, and T. Ikeda, J. Electroanal. Chem. 535 (2001) 37.

Chapter 4

Role of a Non-Ionic Surfactant in Direct Electron Transfer-Type Bioelectrocatalysis by Fructose Dehydrogenase

The author proposes a model to explain the phenomenon as follows. The surfactant forms a monolayer on the hydrophobic MEtn-modified electrode with strong hydrophobic interaction and FDH adsorbs on the surface of the surfactant monolayer. The situation elongates the distance between FDH and the electrode surface to inhibit the electron transfer. On the other hand, the surfactant forms a bilayer on the hydrophilic MEtOH-modified electrode. The interaction between the surfactant bilayer and the hydrophilic electrode is relatively weak so that FDH replaces the surfactant and is embedded in the bilayer to communicate electrochemically with the hydrophilic electrode.

Introduction

Redox enzymes catalyze the electron transfer from the first substrate to the second substrate, and are involved in many vital processes including glycolysis process, tricarboxylic cycle, respiratory chain, and photosynthetic process [1,2]. Enzymes have the substrate specificity and recognize intrinsic substrate *in vivo*. However, the substrate specificity for one of the two substrates is frequently not so high for almost all redox enzymes. Therefore, they can react with artificial electron acceptor (or donor) *in vitro*. The redox enzyme reactions can be combined with electrode reaction, because the artificial electron acceptor (or donor) is reoxidized (or rereduced) at electrodes [3-5]. Furthermore, a limited number of enzymes can directly transfer electron to (or from) electrode [6-14]. The former and latter are called mediated (MET) and direct electron transfer (DET)-type bioelectrocatalysis reaction, respectively. Both reactions are utilized to construct bioelectrochemical devices, such as biofuel cells and biosensors [5,7,15-17]. MET-type bio-devices might be superior in part to DET-type ones in the perfomance, since most of DET-type enzymes show rather low activity for electrodes. However, DET-type bioelectrocatalysis reaction attracts great attention, because it avoids several problems concerning mediator [15-18]. It has been proposed that the following two characteristics are essential to realize DET-type bioelectrocatalysis [19]. One is that the enzyme has more than two redox centers. The other is that one of the redox centers is located near the enzyme surface to act as a built-in mediator for the fast

electron transfer between the enzyme and electrode. There must exits another factors governing DET reaction. However, it is extremely difficult to find novel common features among DET-type enzymes.

A cofactor in DET-type enzymes generally transfer electrons from (or to) electrode. Multi-copper oxidases, such as laccase [8], Cu efflux oxidase [10] and bilirubin oxidase [20], are reported to act as DET-type enzymes for oxygen reduction. These enzymes commonly have a type 1 copper center and a type 2-3 copper cluster. On the other hand, DET-type enzymes for substrate oxidation have various cofactors, such as flavins, quinones, hemes and iron–sulfur clusters. The author has focused membrane-bound enzymes as a model group of DET-type enzymes for anodes, since a variety of membrane-bound enzymes including hydrogenase [11,12], gluconate dehydrogenase [13], and alcohol dehydrogenase [14] show high DET-type bioelectrocatalytic activity.

D-Fructose dehydrogenase (FDH; EC 1.1.99.11) from *Gluconobacter japonicus* NBRC3260 is a heterotrimeric membrane-bound enzyme. The author has succeeded in constructing an overexpression system of FDH [21]. Subunits I and II have covalently bound flavin adenine dinucleotide (FAD) and three heme C moieties, respectively, while the function of subunit III is not clear at the present moment [21,22]. FDH shows strict substrate specificity to D-fructose and is used in diagnosis and food analysis [23,24]. FDH is one of the redox enzymes capable of DET-type bioelectrocatalysis [25], and gives very large current density of DET-type fructose oxidation at a large variety of electrodes [20,26-28]. The FAD is the catalytic site to accept electrons from the substrate, and the electrons are transferred to electrodes through the heme C [29]. The subunit II is essential in the fast electron transfer from the solubilized FDH to electrode as well as ubiquinone derivatives. For further discussion on the electron transfer pathway, some structural information will be required, but no information is available on the crystal structure of FDH at the present moment.

On the other hand, effective DET reaction should require proper orientation such that the heme C moiety of FDH faces to electrode in a short distance to directly and quickly transfer electrons to electrode. Several surfactants are often used to avoid non-specific adsorption of proteins [30,31] and then seem to more or less inhibit the DET-type bioelectrocatalysis due for example to preferred adsorption of the surfactant over the enzyme. However, some non-ionic surfactants such as Triton® X-100 are required in solubilization of membrane-bound FDH from the membrane fraction. Subunit II containing three heme C moieties seems to be

the membrane-anchoring moiety. The surfactant seems to adsorb on the membrane-anchoring region of the solubilized FDH. Considering the fact that FDH gives large catalytic current density in DET-type bioelectrocatalysis even in the presence of Triton® X-100 at several electrodes such as carbon electrodes [25], the surfactant might have an important role to adsorb FDH in a manner suitable for DET-type bioelectrocatalysis.

In this paper, the author focuses the attention on effects of Triton® X-100 on the DET-type bioelectrocatalysis caused by FDH. Au(111) is used as an electrode material, since the surface is sufficiently flat and the surface property is easily tuned by modification with several thiol molecules to fabricate self-assembled monolayer (SAM) [32]. The author constructs two kinds SAM-Au(111) electrodes with 2-mercaptoethanol (MEtOH) and mercaptoethane (MEtn) as hydrophilic and hydrophobic surface-containing electrodes, respectively. In addition, the author focus on the change in the catalytic current density in the bioelectrocatalytic current measurements as well as the frequency shift in quartz crystal microbalance (QCM) measurements as measures of the orientation, the distance, and the surface concentration of FDH on the electrodes. The author proposes a model of the adsorption of the surfactant and FDH to reasonably explain the experimental results.

Experimental

Chemicals

MEtOH was purchased from Nacalai tesque (Japan). Other chemicals including MEtn and Triton® X-100 were from Wako Pure Chemical Industries (Japan). The expression and purification of FDH were carried out as described previously [21,22]. The fructose oxidation activity of solubilized FDH was measured spectrophotometrically with potassium ferricyanide and the ferric dupanol reagent, as described previously [22].

Preparation of electrodes

Au(111) electrodes were prepared on freshly cleaved mica surface by vapor deposition at less than 6.5×10^{-4} Pa. The temperature of a mica sheet was maintained at 580 °C during the deposition. Au-deposited mica sheets were subsequently annealed at 580 °C for 8 h and then quenched in ultrapure water.

SAM-modified Au(111) electrode was prepared by immersing the Au-coated

mica substrates for at least 1 h in an ethanol solution containing 1 mM of the corresponding thiol. Before measurements, SAM-modified Au(111) electrode was washed thoroughly with ethanol and ultrapure water in turn.

Electrochemical measurements

Cyclic voltammetry and chronoamperometry were carried out in McIlvaine buffer (pH 5.0) at 25 °C with a BAS CV-50W electrochemical analyzer under anaerobic conditions. The working electrode was the Au(111) electrode, of which the projected surface area was 0.283 cm^2. The reference and counter electrodes were a handmade Ag|AgCl|sat.KCl electrode and a Pt wire, respectively. All the potentials in this paper are referred to the reference electrode.

QCM measurements with Au electrodes

QCM measurements were performed on a Seiko EG&G QCA917 QCM analyzer at the room temperature. 9-MHz At-cut quartz crystal plates were used (Seiko EG&G Co., Ltd.), of which the projected surface area was 0.196 cm^2.

Results and discussion

Catalytic currents at hydrophobic and hydrophilic electrodes in the absence of the surfactant

FDH was purified according to the literature [21,22]. The purified FDH solution contained 0.1% (W/W) Triton® X-100. Two μL of FDH solution (40 μM) was added into 1 mL of the electrolytic test solution to adsorb FDH on the electrodes in this work, unless otherwise stated. The final surfactant concentration of Triton X® -100 (0.0002%) is sufficiently lower than the critical micelle concentration (CMC, 0.3 mM (0.02%)) [33]. Bioelectrocatalytic current measurements were performed in the McIlvaine buffer (pH 5.0) containing 200 mM fructose. The author used two types of thiols for constructing SAM on the Au(111) electrodes. The surfaces of MEtOH- and MEtn-modified electrodes are hydrophilic and hydrophobic, respectively.

Fig. 1, panel A shows cyclic voltammograms (CVs) of FDH-catalyzed fructose oxidation at MEtn- and MEtOH- SAM-modified and bare Au(111)electrodes. Fructose oxidation catalytic currents were observed at all of the electrodes examined, but hydrophilic MEtOH-modifed Au electrode gave much larger current density compared with hydrophobic MEtn-modified Au electrode. Furthermore, the

MEtn-modified electrode showed low stability in the DET-type bioelectrocatalytic reaction (Fig. 1, panel B): multiple scanning in cyclic voltammetry caused a gradual decrease in the catalytic current. Similar phenomenon was observed at hydrophobic Au (111) electrode modified with benzenthiol (data not shown). In contrast, the current response at MEtOH-modified electrode was very stable during multiple scanning. Since clear frequency shift was not observed in QCM measurements during the potential scan at FDH-adsorbed MEtn-modified Au electrode (data not shown), the decrease in the catalytic current would not be attributed to the desorption of FDH from the electrode surface. Some denaturation might occur at such hydrophobic electrode surface during the potential scan especially at positive potentials [34]. In addition, the MEtn-modified electrode provided strange characteristics: the catalytic current in the forward positive-going scan was smaller than that in the backward negative-going scan (Fig. 1, panel B). However, the reason is not clear.

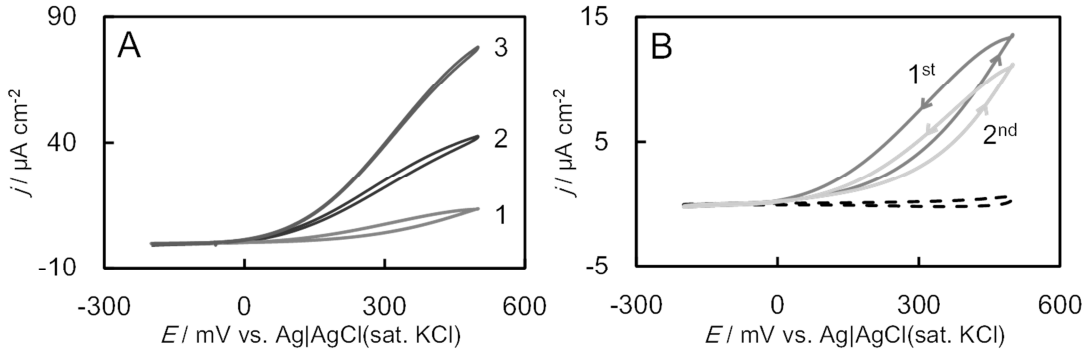

Figure 1. (A): CVs of fructose oxidation catalyzed by FDH adsorbed on (1) MEtn-modified, (2) MEtOH-modified, and (3) bare Au electrode in the presence of 200 mM fructose.
(B): Multi-scan CVs at FDH-adsorbed MEtn-modified electrode (broken black line) in the absence and (1st cycle and 2nd cycle) presence of fructose (200 mM). All CVs were recorded at pH 5.0 and ν = 10 mV s^{-1}.

Effects of the surfactant adsorption on the DET-type catalytic current

The question here is whether FDH and the surfactant adsorb competitively or cooperatively on the electrodes. Therefore, the author examined effects of the surfactant addition on the fructose oxidation current catalyzed by adsorbed FDH.

After the addition of FDH in the test solution (and then adsorption of FDH on the electrodes), chronoamperometric monitoring of the catalytic current was performed at 500 mV. After the current reached a steady state, Triton® X-100 solution was added in the electrolysis solution and the current response was monitored (surfactant post-addition experiments). The concentration of the surfactant was set at 1% as a final concentration, because it is identical with that set for the solubilization of FDH from the membrane fraction [21]. At this concentration of the surfactant, about 70% of FDH is solubilized from the membrane fraction by gentle stirring in MacIlvaine buffer (pH 6.0) for 1 h at 4 °C (Data not shown). In addition, the specific activities of FDH in the presence and absence of 1% Triton® X-100 were 160 ± 20 U mg^{-1} and 180 ± 12 U mg^{-1}, respectively. Thus, the author can conclude that there is no significant difference in the specific activity of FDH between in the presence and absence of 1% Triton® X-100 ($p > 0.1$, Student's t test; $n = 6$). Note here that the expression of "the absence of 1% Triton® X-100" in this paper does not mean the complete absence of the surfactant, but 0.0002% of the surfactant, as above described.

The chronoamperometric data are given in Fig. 2, panels A–C. At hydrophobic MEtn-modified electrode, the catalytic current was decreased down to almost zero immediately after the addition of the surfactant (panel A). The result suggests that FDH and the surfactant adsorb strongly competitively on the hydrophobic electrode surface. In contrast, at hydrophilic MEtOH-modified electrode, the catalytic current retained about 80% of that before the addition of the 1% surfactant (panel B). Medium response was observed at the bare Au electrode (panel C).

The inset of Fig. 2, panel D shows CVs of FDH-catalyzed fructose oxidation at the MEtOH-modified electrode before and after the addition of the 1% surfactant. The surfactant addition caused only small decrease in the catalytic current, as in the case of the chronoamperometric measurements (Fig. 2, panel B), but the shape of the current-potential curve remained unchanged, as evidenced by the normalized CVs depicted in panel D. By considering the property of the current-potential curve of DET-type bioelectrocatalysis in the presence of excess substrate [35], the complete coincidence of the two normalized CVs before and after the addition of the surfactant indicates that the addition of the surfactant (1%) causes only slight decrease in the surface concentration of properly oriented FDH on the hydrophilic electrode surface, but the electrode and enzymatic kinetics remained unchanged on the surfactant addition.

The author also recorded CVs of FDH-catalyzed fructose oxidation at the SAM-modified electrodes in the presence of 1% Triton® X-100 before the addition of FDH (Fig. 3, surfactant pre-addition experiments). At the hydrophobic MEtn-modified Au electrode, no catalytic current was observed (panel A). The result also indicates that Triton® X-100 adsorbs predominantly on the hydrophobic electrode to inhibit the DET-type bioelectrocatalysis.

In contrast, the addition of FDH caused the appearance of clear catalytic wave at the hydrophilic MEtOH-modified Au electrode even in the presence of the surfactant (1%), as shown in panel B. The current density was almost identical with that observed in the surfactant post-addition experiments described before (dashed lined in the inset of Fig. 2, panel D). At the bare Au electrode, the catalytic wave was observed, but the current density was much smaller than that at the MEtOH-modified electrode. The effect of the pre-addition of the surfactant on the current was similar to that of the post-addition experiments.

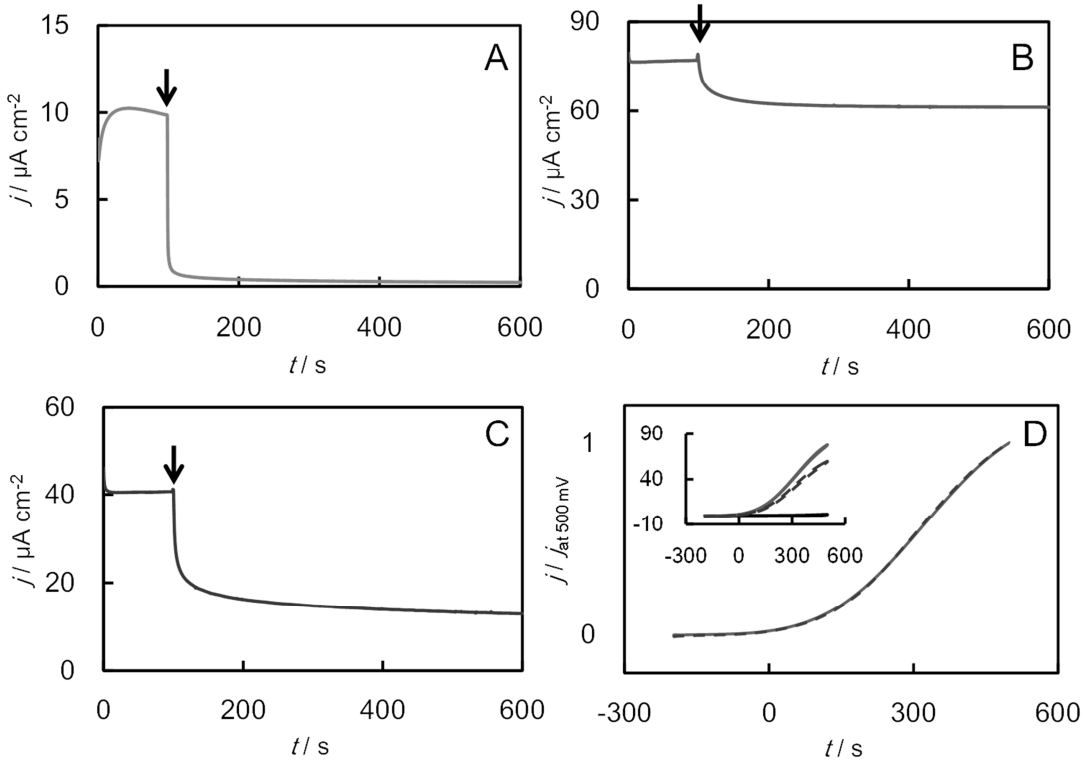

Figure 2. DET-type FDH-catalyzed current response in the presence of 200 mM fructose.

(A-C) Chronomperometric response on MEtn-modified (A), MEtOH-modified (B), and bare (C) Au(111) electrode at 500 mV. 1% Triton® X-100 was added to the electrolysis solution at the point indicated by the arrow.

(D): Relative current expression of CVs of FDH-catalyzed fructose oxidation at MEtOH-modified Au(111) electrode before (solid line) and after (dashed line) the addition of 1% Triton® X-100. The current is normalized against the value at 500 mV. The inset shows the original CV data, in which the black solid line is the background CV.

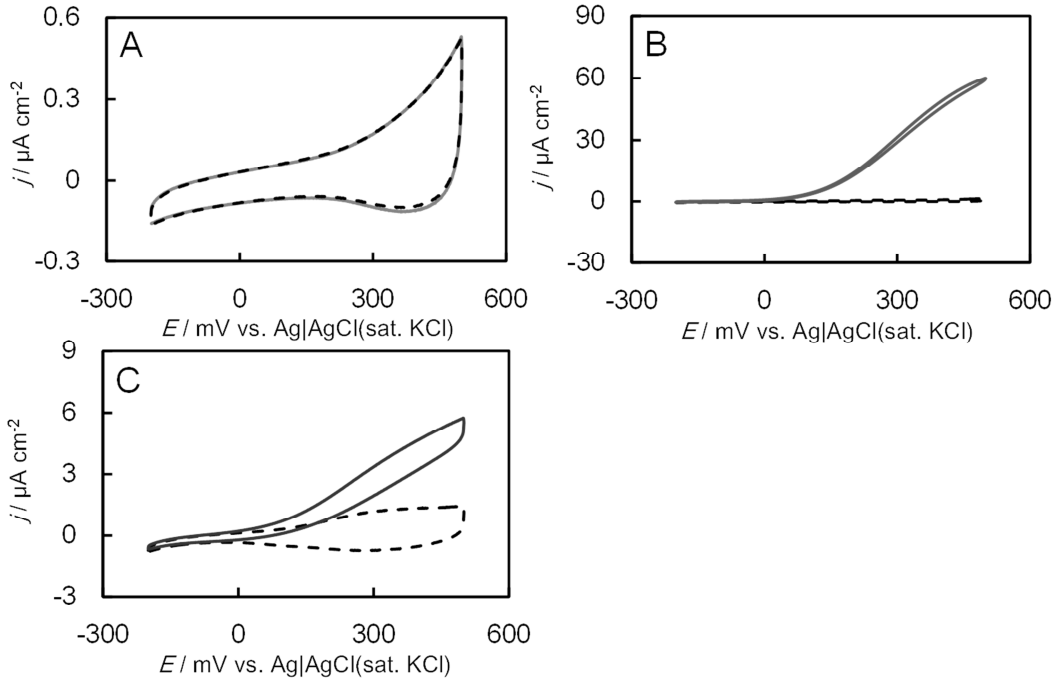

Figure 3. CVs of fructose oxidation catalyzed FDH adsorbed on (A) MEtn-modified, (B) MEtOH modified, and (C) bare Au(111) electrodes in the presence of 200 mM fructose and 1% Triton® X-100. All CVs were performed at pH 5.0 and ν = 10 mV s^{-1}. The background CVs (in the absence of fructose) are given by the broken curves.

QCM measurements and adsorption model

The adsorption of the surfactant and FDH on the electrode was monitored on QCM. We first added 1% Triton® X-100 into the test solution, and after the current reached a steady state, the author succeedingly added FDH. The time course of the resonance frequency (*f*) is given in Fig. 4. At the MEtn-modified electrode, the *f* value decreased immediately after the addition of Triton® X-100 at the position indicated by the solid arrow (curve A), indicating the strong adsorption of the surfactant on the hydrophobic surface most probably to form monolayer on the hydrophobic surface. The succeeding addition of FDH at the position indicated by the dashed arrow also decreased the *f* value, indicating the adsorption of FDH. By considering the complete inhibition of the DET-type bioelectrocatalysis by the surfactant addition and the strong attractive interaction between the surfactant and the hydrophobic surface, FDH most probably adsorbs on the monolayer of the

surfactant, as illustrated in Fig. 5 (A).

It is reported that non-ionic surfactants form monolayer on hydrophobic surface at high concentrations of the surfactants [36,37] in such a manner that the hydrophobic tail groups of the surfactant anchor to the hydrophobic surface and the hydrophilic head groups face the solution. The limiting value of the frequency shift (Δf) on the addition of Triton® X-100 was about –40 Hz at the MEtn-modified Au(111) electrode (Fig. 4, curve A), which corresponds to a mass change per unit area ($\Delta m / A$) of 2.0×10^2 ng cm^{-2} according to Sauerbrey equation [38].

$$\Delta f = -\frac{2 f_0^{\,2} \Delta m}{A\sqrt{\mu_q \rho_q}} \qquad (1)$$

where f_0 is the fundamental resonance frequency (9 MHz), μ_q is the shear module (2.947×10^{10} kg m^{-1} s^{-2}), ρ_q is the density of the quartz (2.648×10^3 kg m^{-3}), respectively. Assuming the monolayer formation of the surfactant and a molecular mass of 650 Da for Triton® X-100 (n = 10, n being the number of the polyethylene oxide group), rough evaluation of the area occupied by one molecule of Triton® X-100 yields 0.8 (nm)^2/molecule. This value is reasonable as a projected area of Triton® X-100 from the axis of the molecule. Therefore, the QCM data support the monolayer formation of Triton® X-100.

It can be expected that the monolayer formation of FDH causes a frequency shift (Δf) of –110 Hz by considering a molecular mass of 140 kDa and an FDH-occupied area of 7 (nm)^2/molecule [26]. This expectation is verified by QCM measurements of the adsorption of FDH on the MEtOH-modified or bare Au(111) electrode in the absence of the surfactant (Fig. 6). The Δf value was about 50 Hz upon the adsorption of FDH on Triton® X-100-monolayer-adsorbed MEtn-modified electrode (Fig. 4, panel A). Therefore, the surface coverage of FDH adsorption layer on the Triton® X-100-monolayer may be calculated to be 0.4 (= 50 Hz/110 Hz). It seems to be difficult to transfer the electron from reduced FDH on the Triton® X-100-monolayer to the Au electrode through the Triton® X-100-monolayer (3-nm thickness) and the MEtn-SAM (0.3-nm thickness), since long range electron transfer kinetics reduces exponentially as increasing the distance between electron donor and acceptor [39,40]. Actually, FDH falls silent in DET-type bioelectrocatalysis at the hydrophobic MEtn-Au electrode in the presence of Triton® X-100 (1%).

Even at the MEtOH-modified Au electrode, the f value decreased immediately after the addition of Triton® X-100 (Fig. 4, curve B). The limiting value

of the frequency shift (Δf) on the addition of Triton® X-100 was about –100 Hz. The result suggests the bilayer formation of Triton® X-100 on the hydrophilic surface. There are a number of studies on the behavior of non-ionic surfactants on silica/liquid interface [41,42]. It has been reported that high concentrations of Triton® X-100 forms bilayer on bare silica in such a manner that the adsorption of Triton® X-100 takes place through the ethoxy group on the silica and that the hydrophobic tail moiety is responsible for the bilayer formation.

On the succeeding addition of FDH into the solution, the frequency decreased gradually with the time, as shown by curve B of Fig. 4, indicating relatively slow adsorption of FDH on Triton® X-100-bilayer-adsorbed MEtOH-modified Au electrode. Considering the fact that the FDH can communicate with the MEtOH-modified Au electrode, as evidenced by Fig. 2, panels B and D and Fig. 3, panel B, the situation can be ruled out that FDH adsorbs directly on the surface of the bilayer of Triton® X-100. A more plausible model proposed here is that FDH inserts into the Triton® X-100 bilayer and replaces parts of the bilayer, as illustrated in Fig. 5 (B). The interaction between the ethoxy group of Triton® X-100 and the hydroxyl group of MEtOH seems to be weak compared with that between FDH and MEtOH-SAM. It is reasonable to consider that the FDH embedded in the Triton® X-100 bilayer communicates with MEtOH-modified electrode in the presence of Triton® X-100. In addition, the situation in the proposed model is close to the native situation of FDH bound to the membrane, and seems to be convenient for FDH. This seems to be supported by the very large and stable response of FDH in DET-type bioelectrocatalysis at the hydrophilic MEtOH-modified Au electrode in the presence of Triton® X-100. The gradual decrease in the frequency on the addition of FDH (Fig. 4, panel B) seems to indicate the slow embedding process of FDH.

The bare Au electrode showed medium QCM response between the hydrophobic MEtn-modified electrode and hydrophilic MEtOH-modified electrode. Most probably, Triton® X-100 forms monolayer predominantly on bare Au electrode, but in only limited parts the bilayer is also constructed to embed FDH.

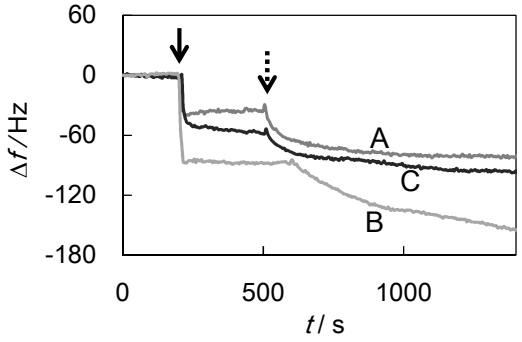

Figure 4. Frequency changes on the addition of 1% Triton® X-100 (at the solid arrow) and FDH (at the dashed arrow) at (A) MEtn-modified, (B) MEtOH-modified, and (C) bare Au electrodes.

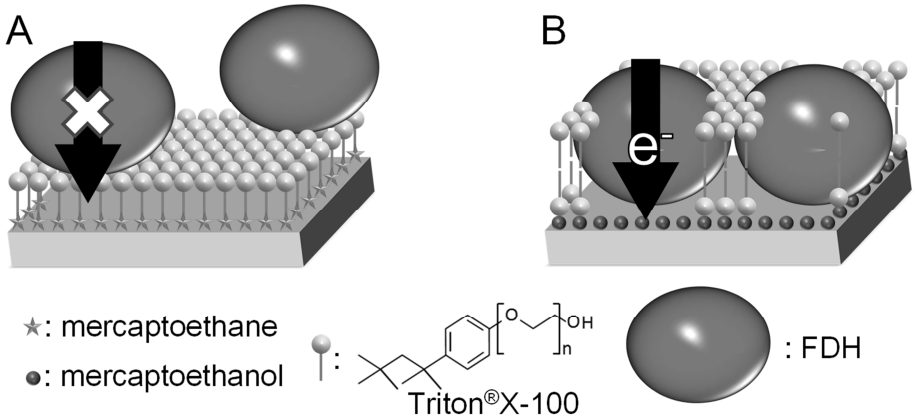

Figure 5. The proposed scheme of the adsorption of FDH and Triton® X-100 at (A) hydrophobic and (B) hydrophilic electrodes.

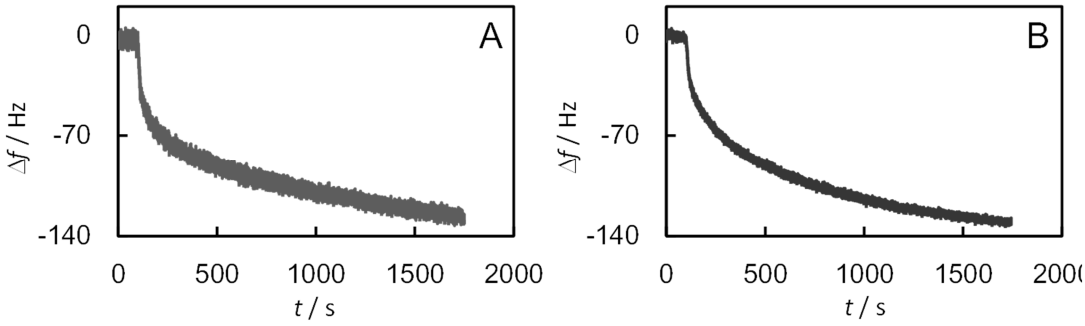

Fig. 6 Frequency changes on the adsorption of FDH in the absence of 1% Triton® X-100 at (A) MEtOH-modified and (B) bare Au electrodes.

References

[1] P. N. Bartlett (Ed), Bioelectrochemistry, John Wiley & Sons Ltd., West Sussex, 2008.

[2] G. W. Canters, E. Vijgenboom (Eds), Biological Electron Transfer Chains: Genetics, Composition and Mode of Operation, Kluwer Academic Publishers, Dordrecht, 1998.

[3] A. Heller, Phys. Chem. Chem. Phys. 6 (2004) 209.

[4] N. Mano, J. L. Fernandez, Y. Kim, W. Shin, A. J. Bard, and A. Heller, J. Am. Chem. Soc. 125 (2003) 15290.

[5] C. Nieh, Y. Kitazumi, O. Shirai, M. Yamamoto, and K. Kano, Electrochem. Commun. 33 (2013) 135.

[6] F. A. Armstrong, Curr. Opin. Chem. Biol. 9 (2005) 110.

[7] L. Gorton, A. Lindgren, T. Larsson, F. D. Munteanu, T. Ruzgas, and I. Gazaryan, Anal. Chim. Acta. 400 (1999) 91.

[8] S. Shleev, J. Tkac, A. Christenson, T. Ruzgas, A. I.Yaropolov, J. W. Whittaker, and L. Gorton, Biosens. Bioelectron. 20 (2005) 2517.

[9] Y. Kamitaka, S. Tsujimura, N. Setoyama, T. Kajino, and K. Kano, Phys. Chem. Chem. Phys. 9 (2007) 1793.

[10] Y. Miura, S. Tsujimura, Y. Kamitaka, S. Kurose, K. Kataoka, T. Sakurai, and K. Kano, Chem. Lett. 36 (2007) 132.

[11] A. Ciaccafava, P. Infossi, M. Ilbert, M. Guiral, S. Lecomte, M. T. Giudici-Orticoni, and E. Lojou, Angew. Chem. 50 (2011) 1.

[12] H. R. Pershad, J. L. C. Duff, H. A. Heering, E. C. Duin, S. P. J. Albracht, and F. A. Armstrong, Biochemistry 38 (1999) 8992.

[13] S. Tsujimura, T. Abo, Y. Ano, K. Matsushita, and K. Kano, Chem. Lett. 36 (2007) 1164.

[14] T. Ikeda, D. Kobayashi, F. Matsushita, T. Sagara, and K. Niki, J. Electroanal. Chem. 361 (1993) 221.

[15] S. C. Barton, J. Gallaway, and P. Atanassov, Chem. ReV. 104 (2004) 4867.

[16] J. A. Cracknell, K. A. Vincent, and F. A. Armstrong, Chem. Rev. 108 (2008) 2439.

[17] K. So, S. Kawai, Y. Hamano, Y. Kitazumi, O. Shirai, M. Hibi, J. Ogawa, and K. Kano, Phys. Chem. Chem. Phys. 16 (2014) 4823.

[18] J. T. Holland, C. Lau, S. Brozik, P. Atanassov, and S. Banta, J. Am. Chem. Soc. 133 (2011) 19262.

[19] T. Ikeda, Direct redox communication between enzymes and electrodes, in: F. W. Scheller, F. Schubert, J. Fedrowitz (Eds.), Frontiers in Biosensorics I, Birkhäuser Verlag Basel, Switzerland, 1997, p. 243.
[20] Y. Kamitaka, S. Tsujimura, T. Ikeda, and K. Kano, Electrochemistry 74 (2006) 642.
[21] S. Kawai, M. Tsutsumi, T. Yakushi, K. Kano, and K. Matsushita, Appl. Environ. Microbiol. 79 (2013) 1654.
[22] M. Ameyama, E. Shinagawa, K. Matsushita, and O. Adachi, J. Bacteriol. 145 (1981) 814.
[23] R. Antiochia, and L. Gorton, Sens. Actuators B 195 (2014) 287.
[24] K. Nakashima, H. Takei, O. Adachi, E. Shinagawa, and M. Ameyama, Clin. Chim. Acta. 151 (1985) 307.
[25] Y. Kamitaka, S. Tsujimura, and K. Kano, Chem. Lett. 36 (2007) 218.
[26] M. Tominaga, C. Shirakihara, and I. Taniguhi, J. Electroanal. Chem. 610 (2007) 1.
[27] K. Murata, M. Suzuki, K. Kajiya, N. Nakamura, and H. Ohno, Electrochem. Commun. 11 (2009) 668.
[28] T. Miyake, S. Yoshino, T. Yamada, K. Hata, and M. Nishizawa, J. Am. Chem. Soc. 133 (2011) 5129.
[29] S. Kawai, T. Yakushi, K. Matsushita, Y. Kitazumi, O. Shirai, and K. Kano, Electrochem. Commun. 38 (2014) 28.
[30] R. Miller, V. B. Fainerman, R. Wüstneck, J. Krägel, and D. V. Trukhin, Colloids. Surf. A 131 (1998) 225.
[31] L. S. Roach, H. Song, and R. F. Ismagilov, Anal. Chem. 77 (2005) 785.
[32] H. Ron, S. Matlis, and I. Rubinstein, Langmuir 14 (1998) 1116.
[33] M. N. Jones, Int. J. Phytorem. 177 (1999) 137.
[34] Y. Sugimoto, Y. Kitazumi, S. Tsujimura, O. Shirai, M. Yamamoto, and K. Kano, Biosens. Bioelectron. 63 (2015) 138.
[35] S. Tsujimura, T. Nakagawa, K. Kano, and T. Ikeda, Electrochemistry 72 (2004) 437.
[36] F. Tiberg, J. Chem. Soc. Faraday Trans. 92 (1996) 531.
[37] L. M. Grant, T. Ederth, and F. Tiberg, Langmuir 16 (2000) 2285.
[38] G. Sauerbrey, Z. Phys. 155 (1959) 206.
[39] H. B. Gray, and J. R. Winkler, Pro. Natl. Acad. Soc. 102 (2005) 3534.
[40] A. Ghindilis, P. Atanasov, and E. Wilkins, Electroanalysis 9 (1997) 661.
[41] G. González, and A. M. Travalloni-Louvisse, Langmuir 5 (1989) 26.

[42] D. M. Nevskaia, M. L. R. Cervantes, A. G. Ruíz, and J. de D. López-González, J. Chem. Tech. Biotechnol. 63 (1995) 249.

Conclusions

D-Fructose dehydrogenase gives direct electron transfer (DET)-type bioelectrocatalysis reaction. FDH has been focused for developing the biodevices, such as biofuel cells and biosensor, because the DET ability of FDH is quite high. However, the mechanism of DET reaction of FDH has been clearly elucidated.

In chapter 1, the author sequenced whole structural genes for the heterotrimeric complex for the first time. The order of the *fdh* genes was the small, cytochrome *c*, and large subunits in the 5′ to 3′direction. The author successfully overexpressed the FDH complex in the *G. oxydans*. Membranes of the cells producing recombinant FDH showed approximately 100-times higher specific activity than those of *G. japonicus* NBRC3260. The specific activity of the purified FDH is 260 units mg^{-1} at 25 °C. The author confirmed that there are three heme C moieties in subunit II (FdhC) and one FAD in subunit I (FdhL).

The work in chapter 2 revealed that the heme C subunit in FDH is essential for the DET-type bioelectrocatalysis of FDH, while D-fructose oxidation proceeds at the FAD redox site even in the absence of the heme C subunit (FdhSL). In FdhSL, the electron is non-specifically transferred from FAD to the quinones and the ET process is the rate-determining step, as evidenced by the LFER characteristics. In contrast, the ET in FDH from the heme C to Q_0 and Q_1 is rather fast and is not the rate-determining step. Some attractive interaction between the heme C moiety and 2,3-dimethoxy-5-methyl-*p*BQ derivatives seems to promote the ET from the heme C site to the quinones. The $E^{\circ\prime}$ values of the three hemes C in FDH have successfully been determined. All of the hemes C can be reduced by D-fructose in the absence of electron acceptors, but heme C_1 with $E_1^{\circ\prime}$ (150 mV) does not seem to be involved in the DET-type bioelectrocatalytic reaction, as judged from $E_1^{\circ\prime}$ of heme C_1 and the onset potential of the DET-type bioelectrocatalytic wave. The author considers that heme C_2 with $E_2^{\circ\prime}$ (60 mV) is the electron-donating site in the DET reaction, as in the case of FDH reaction in the membrane. Since it is not reasonable to assume any specific interaction between heme C_2 and electrode surface, the location of heme C_2 seems to be the most important factor to govern the DET reaction.

The author has constructed the expression system of heme C subunit of FDH (FdhC) in chapter 3. The non-turnover signal of FdhC is not observed on the CV. However, the mixing solution of FdhSL and FdhC shows the fructose-oxidation current. FdhC does not have the fructose-oxidation activity. In contrast, FdhSL has the fructose-oxidation activity, because the FAD in FdhL subunit of FDH is the catalytic center for fructose. The author confirmed with the spectroscopical measurement that FdhSL transfers the electron from fructose to FdhC. These results strongly suggest that FdhC reacts with electrode directly, when there are both FdhSL and

FdhC in the electrochemical measurement solution. In addition, FdhSL and FdhC are bound and work as a one enzyme by mixing of them. This means that the fructose-oxidation current observed by the mixing of FdhSL and FdhC is from DET-type reaction of FDH. The size of FdhC is evaluated as approximately 230 kDa by gel filtration column chromatography. The value is equal to tetramer or more multimer of FdhC. On the other hand, judging from the size of FDH determined by gel filtration column chromatography, FDH forms dimer. The excessive aggregation of FdhC might have bad effect on DET reaction.

In chapter 4, the author controlled the electrode surface hydrophobicity by using two types of SAMs to examine the effect of Triton® X-100 on DET-type bioelectrocatalysis of FDH. In the presence of the surfactant, the hydrophobic MEtn-modified electrode shows no response of DET reaction of FDH in spite of the adsorption of FDH on the MEtn-modified electrode. The author proposes a model in which the surfactant monolayer is formed on the MEtn-modified electrode and FDH adsorbs on the surfactant monolayer. The distance between the redox site of FDH and the electrode surface would be too long to transfer the electron directly. In contrast, FDH is capable of DET-type communication with the hydrophilic MEtOH-modified electrode in the presence of 1% Triton® X-100. The surfactant bilayer is formed on the MET-modified electrode. The interaction between the surfactant layer and the MEtOH-modified electrode is so weak that FDH can replace the bilayer in part and be embedded in the bilayer on the surface of the electrode

The present works can help to plan further studies aiming to engineer some related enzymes for increasing the DET capability. The proposed model on the adsorption of the adsorption of the surfactant and FDH is very important to consider the role of non-ionic surfactants in DET-type bioelectrocatalysis, especially, of membrane-bound redox enzymes.

Acknowledgements

I would like to express my sincere gratitude to Dr. Kenji Kano, Professor of Kyoto University, of his kind guidance and important suggestions throughout this study. Prof. Kano has introduced me to the field of bioelectrochemistry and instructed me in the spirit, “楽しめ、考えろ” throughout all my studies for six years.

I extremely appreciate to Dr. Kazunobu Matsushita, Emeritus Professor of Yamaguchi University, and Dr. Toshiharu Yakushi, Associate Professor of Yamaguchi University for their kind helps, guidance in culture of bacteria, cloning of the gene encoding fructose dehydrogenase and meaningful advices. I had very enjoyable time and valuable experiences at their laboratory.

I am grateful to Dr. Osamu Shirai, Associate Professor of Kyoto University, Dr. Yuki Kitazumi, Assistant Professor of Kyoto University, and Dr. Seiya Tsujimura, Associate Professor of Tsukuba University for their kind advices, supports and comments.

I show my appreciation to Dr. Jun Ogawa, Professor of Kyoto University, and Dr. Shigenobu Kishino, Assistant Professor of Kyoto University for their kind guidance on the work of French Press and a lot of encouragement, and also to Dr. Hideto Miyoshi, Professor of Kyoto University, Dr. Masatoshi Murai, Assistant Professor, and Dr. Masato Abe, Assistant Professor of Kyoto University, for their important advice, guidance on the work of ultracentrifugation, a number of kindness and encouragement.

I gratefully thank Dr. Maiko Goda-Tsutsumi for her technical assistances, helpful suggestion and valuable discussion and encouragement. Inspired by her attitude for her study, I was planning to proceed to doctoral degree. I thanks to the members in Kano laboratory, Mr. Katsumi Hamamoto, Dr. Stefano Freguia, Dr. Shiue-Lin Li, Mr. Shintaro Kubota, Mr. Ryota Kontani, Mr. Kenta Sagara, Mr. Keisuke Sasakura, Ms. Yumi Matsuda Mr. Mr. Masahimi Asahi, Mr. Tsukasa Inoue, Mr. Noriyoshi Ueya, Mr. Takafumi Yamauchi, Dr. Tatsuo Noda, Dr. Chi-Hua Nieh, Dr. Bo-Quan Sha, Mr. Yuki Kushida, Ms. Sae Hamada, Mr. Akihiro Maruyama, Mr. Daichi Mori, Mr. Noriyuki Yamazaki, Mr. Hajime Yamada, Mr. Hiroki Kagohashi, Mr. Masahiro Takeshige, Mr. Rui Hamamoto, Ms. Kanako Hamano, Mr. Wei-Cheng Chen, Ms. You-Xuan Gao, Mr. Keisuke Kimura, Mr. Kento Sakai, Mr. Issei Hirata, Mr. Masahiro Hori, Mr. Yoshinari Takano, Mr. Yutaka Takeuchi, Mr. Yuya Hibino, Mr. Masaki Motoike, Mr. Arato Suzuki, Mr. Riku Usami, Mr. Ryutaro Katsube, Mr. Ryosuke Takeuchi and Mr. Takuya Yamaguchi for their kind supports in my laboratory life in Kyoto University. Also special thanks to Ms. Toshie Koyama, Mr. Yu Sugimoto, Mr. Itaru Asano, Ms. Yuko Kikuchi, Ms. Michiko Shinmura, Mr. Yasuyuki Hamano, Mr. Kei Hichiri and Mr. Keisei Sou for significant discussion, great times in my laboratory life and interesting conversations with them.

Acknowledgements

I give my great appreciation to Dr. Sohrin Kihara, Emeritus Professor of Kyoto Institute of Technology and Kyoto Institute for Interesting Chemistry for kind supports and encouragement, interesting advices and great experience. I also highly appreciate to Dr. Tokuji Ikeda, Emeritus Professor of Kyoto University for valuable discussion and encouragement.

I thanks to members of the polarographic society of Japan, especially to Dr. Kohji Maeda, Professor of Kyoto Institute of Technology, Dr. Masahiro Yamamoto, Professor of Konan University, Dr. Takamasa Sagara, Professor of Nagasaki University, Dr. Masato Tominaga, Associate Professor of Kumamoto University, Dr. Hirosuke Tatsumi, Associate Professor of Shinshu University, Dr. Naoya Nishi, Associate Professor of Kyoto University, and Dr. Yumi Yosida, Associate Professor of Kyoto Institute of Technology for their advice, kindness, encouragement and interesting discussion during the meeting.

I thank professors, doctors and friends, I have ever seen in conferences and events for their kind advices and encouragement.

Finally, I express my greatest appreciation to my family for continuous encouragement.

Shota Kawai
Kyoto
March 2015

List of publications

1) S. Kawai, M. Tsutsumi, T. Yakushi, K. Kano, and K. Matsushita
Heterologous Overexpression and Characterization of a Flavoprotein-Cytochrome *c* Complex Fructose Dehydrogenase of *Gluconobacter japonicus* NBRC3260
Appl. Environ. Microbiol., **79**, 1654-1660 (2013)
(Chapter 1)

2) S. Kawai, T. Yakushi, K. Matsushita, Y. Kitazumi, O. Shirai, and K. Kano
The electron transfer pathway in direct electrochemical communication of fructose dehydrogenase with electrodes
Electrochem. Commun., **38**, 28-31 (2014)
(Chapter 2)

3) S. Kawai, T. Yakushi, K. Matsushita, Y. Kitazumi, O. Shirai, and K. Kano
Role of a non-ionic surfactant in direct electron transfer-type bioelectrocatalysis by fructose dehydrogenase
Electrochim. Acta., **152**, 19-24 (2015)
(Chapter 4)

4) S. Kawai, T. Yakushi, K. Matsushita, Y. Kitazumi, O. Shirai, and K. Kano
Electrochemical characterization on the reconstruction of the subunits of heterotrimeric fructose dehydrogenase
In preparation.
(Chapter 3)